

Accepted Manuscript

Thermoplastic starch wastes are converted and stored into acetone through butanol in a depressurised digester

Sung T. Oh, Alastair Martin, Soo-Jung Kang

PII: S1385-8947(17)32029-6
DOI: <https://doi.org/10.1016/j.cej.2017.11.107>
Reference: CEJ 18078

To appear in: *Chemical Engineering Journal*

Received Date: 18 October 2017
Revised Date: 19 November 2017
Accepted Date: 20 November 2017

Please cite this article as: S.T. Oh, A. Martin, S-J. Kang, Thermoplastic starch wastes are converted and stored into acetone through butanol in a depressurised digester, *Chemical Engineering Journal* (2017), doi: <https://doi.org/10.1016/j.cej.2017.11.107>



This is a PDF file of an unedited manuscript that has been accepted for publication. As a service to our customers we are providing this early version of the manuscript. The manuscript will undergo copyediting, typesetting, and review of the resulting proof before it is published in its final form. Please note that during the production process errors may be discovered which could affect the content, and all legal disclaimers that apply to the journal pertain.

Thermoplastic starch wastes are converted and stored into acetone through butanol in a depressurised digester

Sung T. Oh^{*1}, *Alastair Martin*², and *Soo-Jung Kang*³

^{*1} School of Science and Engineering and Technology, University of Abertay Dundee, DD1 1HG, United Kingdom

² Department of Chemical Engineering, Lancaster University, Bailrigg, Lancaster, LA1 4YR, United Kingdom

³ Department of Polymer Science and Engineering, Sungkyunkwan University, Republic of Korea

AUTHOR EMAIL ADDRESS: ^{*1} s.oh@abertay.ac.uk; ² a.martin1@lancaster.ac.uk; ³

soojung@skku.edu

AUTHOR ADDRESS

^{*1} Sung T. Oh

School of Science and Engineering and Technology, University of Abertay Dundee, Dundee, DD1 1HG, United Kingdom, Tel: +44 1382 308930; E-mail: s.oh@abertay.ac.uk

² Alastair D Martin

Department of Chemical Engineering, Lancaster University, Bailrigg, Lancaster, LA1 4YR, United Kingdom, Tel: +44 1524 592335; E-mail: a.martin1@lancaster.ac.uk

³ Soo-Jung Kang

Department of Polymer Science and Engineering, Sungkyunkwan University, Suwon, 16419, Republic of Korea Tel: :+82-31-290-7301; E-mail: soojung@skku.edu

ABSTRACT

A biofilm containing both *hydrolytic fermentative bacteria* and *acidogenic bacteria* (including *acetogenic* and *acetoclastic bacteria*) was developed for the treatment of plastic wastes in a two-phase, batch digester. The biotransformation and further degradation were electrochemically observed. It was found that the organic wastes were initially fermented in a single-phase (i.e. liquid phase) digester, where it entirely obeyed microbial growth kinetics in accumulating acetate. As the carbonates produced were vaporised, the single-phase became a two-phase fermentation (gas and liquid) accumulating volatile fatty acids (VFAs), where it obeyed a proton driving force based on Le Chatelier's principle. Interestingly, as the digester was depressurised to the saturated vapour pressure of water, the accumulated VFAs were rapidly transformed into acetone *via* butanol, so that the VFAs forms were not observable. It was found that in extreme conditions, the organic feeds were converted and stored into acetone, *via* butanol.

KEYWORDS

Maltose and Starches Fermentation; Anaerobic Digestion; Pressure Dependence; Thermodynamics, Bio-plastics Degradation, Butanol and Acetone Biotransformation

1. INTRODUCTION

Plastics has become a substantial part of our life, and is used in all industries: packaging (39.9 % of all applications), home-ware applications (22.4 %), building & construction (19.7 %), automotive (8.9 %), electrical and electronic devices and tools (5.8 %), and agriculture (3.3 %) [1]. In 2015, the plastics industry produced about 322 million tonnes annually (Bie, 2017), and the EU, US and China mainly shared the world market with 15.8, 15.8, and 27.8 % respectively [1]. It is not surprising that for the last three years, approximately 85 % of the annual production [2] was returned as wastes, but the proportion of recycling of the wastes was significantly reduced. In the UK, about 5 million tonnes of plastic wastes [3] was produced annually, and about 71 % of the wastes was disposed of in landfill sites. In the severe case of the US in 2014,

33.6 million tonnes of the plastic wastes was produced, and approximately 85.5 % of the production [4] was disposed of in landfill sites.

While the plastics industry is expected to face continuous growth, landfill sites in the UK will run out within the next few years [5]. Waste-to-energy (WTE) incineration promises the best option for landfill management reducing landfill tariffs [6], and it also earns revenue from generating electric/heat power regardless of the accompanying air pollution (i.e. dioxin or mercury). However, it requires a strict dried condition in a range of less than 65 % of water content, which pays for tremendous thermal energy in the pre-treatment processes, and or selective collection programmes of the wastes. Besides, the financial viability has become strongly dependent on the Feed-in Tariffs schemes, since the price of oil has fallen to the point of 70 % below the 2014 price [7]. However, there is no doubt that recycling is still the best option for dealing with plastic wastes.

Much attention has been paid to anaerobic digestion (AD) [8] in the recycling of biodegradable wastes, and it has been shown to be more cost-effective than WTE in the range of (85–95) % water content. The technology can also transform plastic wastes to renewable energy, such as biogas. However, AD *in nature* is a slow and complicated process with three major microbial stages: (i) hydrolytic fermentative stage, (ii) acidogenic stage, and (iii) methanogenic stage. Membrane baffled reactors have been applied in lab-based experiment, for separation of the microbial stages from the single AD process [9, 10]. However, the microbial AD stages are entirely integrated by themselves, and they are dissociated and associated with the other stages to produce and utilise ATP energy as the wastes decompose. In the first stage of hydrolysis, *fermentative bacteria* attach to a complex plastic particle [11], where they produce extracellular enzymes to hydrolyse the solid matter, and then convert the soluble products (i.e. glucose, long chain fatty acids, amino acids and other organic acids) into fermentation products (i.e. ethanol, lactic acid, short chain fatty acids, benzoate, formate, and/or carbon dioxide) for maintenance of their cells [12]. As the products, such as ethanol (>11 % w/w), accumulate in the broth, cell lysis is induced in most bacterial species including *Escherichia coli*. This significantly impacts the cell membranes of *hydrolytic fermentative bacteria*, and inhibits the production of extracellular hydrolytic enzymes [13]. This effect, which is readily observed in alcoholic fermentation, is thermodynamically favourable ($\Delta G < 0$ and $\Delta H < 0$). However, it predominantly relies on bacterial attachment (i.e. acclimatisation) on the plastic particles, and often requires donors of electron and

proton [14]. Some fermentative products are further biodegraded to a variety of organic acids, which are simultaneously decomposed to acetate by *acidogenic bacteria*. They are relatively passive donors of electron and proton to *fermentative bacteria*, and they are also activated by thermal energy with regard to ATP energy. This second stage is theoretically reversible, but it always observes a thermodynamic limitation ($\Delta G > 0$ and $\Delta H > 0$). In this case, both these first and second stages are readily able to bond spontaneously by themselves and build a two-layer structured (fermentative-acidogenic) biofilm [15], which can readily be observed in acid-fermentation on organic particles.

The microbial biofilm in AD has massive potential to transform plastic wastes to platform chemicals. Many researchers [16-18] have extensively studied the transformation of thermoplastic starch wastes to polyhydroxyalkanoates (PHA). Russo *et al.* [19] also observed the biodegradability of thermoplastic starch wastes blending polymeric substance (Polyvinyl Alcohol). Biodegradability of 60 % (by weight) was achieved for a 90:10 (Starch:PVA) blend, 40 % for 75:25, 30 % for 50:50, and 15 % for PVA only, respectively. In the case of *Clostridium acetobutylicum*, the biofilm [20-22] was used to transform the thermoplastic starch wastes to PHA, where over 95 % in degradability with 68.7 % conversion of the cell dry weight was achieved within 700 hours. *Clostridium diolis* biofilm [23] was also observed to transform a plastic monomer (i.e. dicarboxylic acids) to ethanol, butanol, and or 1,3-propanediol. The product ratio through metabolic pathway was initially in various ranges [24], but rapidly shifted to produce 1,3-propanediol only. Butanol transformation of the plastic wastes [25-27] in the AD process has also been studied in a hetero-fermentation (i.e. AD without a methanogenic stage) but is not satisfied at the productivity (< approximately 10 g/l) for the industrial viability. The former which mentioned operation parameters led industrial biofilm technologies in the biotechnology. As an example of the work, Li *et al.* [28] studied a biofilm containing *Clostridium beijerinckii* and *Clostridium tyrobutyricum* in a fibrous-bed bioreactor (FBB) for the enhancement of a production of butanol from glucose. Other researchers [29, 30] investigated a membrane-pervaporation with a batch digester converting cassava waste into butanol.

In this manuscript, a biofilm containing the (i) hydrolytic fermentative stage, and (ii) acidogenic stage, including acetogenic and acetoclastic processes, was electrochemically investigated for the biotransformation of thermoplastic starch wastes. Maltose was a model compound in the thermoplastic starch wastes, and it was transformed to volatile fatty acids (VFAs) in a single-

phase batch AD without *methanogenic bacteria*. As the carbonates produced increased, the single-phase was converted into two-phase AD. In this manuscript, the microbial association/dissociation between the first and second stages is clearly explained, and the thermodynamic behaviour in the phase transition is also explicitly described with empirical observations, of which the data are further discussed, together with empirical observations of fermentations in palmitic oil waste, cassava waste, and lactose waste, respectively. The observations show qualitative and qualitative agreement with the model data. Interestingly, it was observed that the microbial association in depressurized biofilm in two-phase AD is suddenly self-transformed into the pathway converting existing VFAs to acetone *via* butanol around the saturated vapour pressure of water. This study identified that a microbial metabolic pathway of VFAs can be bypassed into acetone *via* butanol, rather than the conventional pathway of converting acetate to carbonates. This study was applied for the overcome of thermodynamic and kinetic limitations, leading to practical operation in the biotransformation of thermoplastic starch wastes. However, the model can be applied to different forms, bioflocs in anaerobic digestion or fermentation, and even cell arrays of eukaryotic cells (i.e. human metabolism including metabolic flux analysis). In industrial cases, the set of model equations can be applied to a study of energetics in ‘syntrophic bacteria community’ in terms of microbial community analysis, which has currently been researched in the food sciences and or the extreme conditions including Arctic, Antarctica, deep sea or volcanic environments.

2. MODEL DEVELOPMENT

A biotransformation of thermoplastic starch wastes was investigated in an anaerobic batch digester, where a biofilm containing both (i) a hydrolytic fermentative stage, and (ii) an acidogenic stage was modelled and simulated in an isothermal and isobaric condition (298.15 K and 1 atm). A two-phase digester was also assumed: gas and solution. The model compound of thermoplastic starch was a maltose. One mmole of aqueous carbon dioxide (CO_2) and 36 mmole of acetate ($\text{C}_2\text{H}_4\text{O}_2$) were injected into the digester, and 130 mmole of aqueous ammonia (NH_3) was also assumed in the approximate range of (10–250) mmole l^{-1} as mixed sewage sludge [31].

The biofilm was assumed to contain a fully acclimatised bacterial consortium without *methanogenic bacteria*: *fermentative bacteria*, *acidogenic bacteria*, *acetogenic bacteria* and

acetoclastic bacteria. The microbial growth was assumed to be at a quasi-steady state; meanwhile, the entire transport phenomena of metabolites were assumed to be at the thermodynamic equilibrium state. The assumption was based on the fundamental knowledge of chemical transport phenomena, which are much faster than the conventional microbial growth kinetics, including cellular differentiation [14, 31]. The microorganisms having anaerobic respiration were also assumed to exchange a couple of intra/extracellular mediators (NAD^+/NADH) [12, 14, 15, 31-33], so as to share their metabolites. One mmole of NADH was added as the mediator, which was further assumed to be used in a citric acid cycle (CAC) and oxidative phosphorylation.

Strict mass conservation (one kg) was applied in the two-phase, batch digester. The absolute pressure was increased from one atm up to the pressure (100 atm) at which a micro-bioreactor [34] usually operated, and it was decreased from one atm down to the pressure (3×10^{-4} atm) at which the liquid phase vanished. Here, the direction and magnitude of thermodynamic driving forces (ΔG , ΔH and ΔS) were observed in the whole equilibria state ($\Delta G = \text{zero}$). The model comprised three parts of the equilibrium state (phase transition, dissociation, and redox reaction of metabolites). The first included equilibrium expressions that relate to the relative aqueous activities and gas fugacities of all metabolite species, and the second consisted of the dissociation/association that quantified the relationships between cation and anion activities in the liquid phase. The third consisted of the reduction and oxidation state that is based on the electrochemical potential (V) through the NAD^+/NADH ratio.

The completed model consisted of a set of highly non-linear simultaneous equations, and it was resolved by Newton-Raphson Algorithm [12, 33], based on the Jacobian matrix. The algorithm was coded in C++ in Microsoft visual studio version 2010, and a convergence criterion was set to 1×10^{-14} (pico-%: relative error/tolerance). The average operating time was 2 min per single set, and the maximum operating time was also set to 5 min per single set with Intel Core 2 Duo T6670 processor \times 64-bit, 8 GB memory and 500 GB storage. The operation parameters (Pressure or Initial mole of maltose feedstock) on each set were increased by 1×10^{-4} .

2.1 Stoichiometric relationship

The stoichiometric expressions were established in common, to quantify the feasible relationships between the initial substrate and the products. Table 1 shows the stoichiometric

relationship for the biotransformation of maltose in thermoplastic starch wastes. The stoichiometric relationships were categorised by three equilibrium relationships, which were the two-phase transition, dissociation, and redox of the metabolites.

<TABLE 1> Stoichiometric model of the biotransformation of maltose.

2.2 Equilibrium relationship

This model from the stoichiometric foundations was developed using the fundamental definition of thermodynamic chemical equilibrium:

$$\sum v_i \mu_i = 0 \quad (1)$$

where, v_i is the stoichiometric coefficient of component i , and the chemical potential μ_i is expressed as the standard chemical potential μ_i° and activity a_i of component i .

$$\mu_i = \mu_i^\circ + RT \ln a_i \quad (2)$$

where, R is the universal gas constant, and T is the absolute temperature.

2.2.1 Phase (Gas and Liquid) equilibrium

The gas and liquid equilibrium relevant to the biotransformation of thermoplastic starch wastes was developed in a conventional fermentation [15, 33]. Isomers of butanol, isomers of propanol, acetone, acetaldehyde, ethanol, methanol, ammonia, nitrogen, hydrogen, carbon dioxide, and water were considered as volatiles, due to the relatively high Henry's coefficients ($>1 \times 10^{-3}$). Most metabolites, including volatile fatty acids, were assumed as non-volatiles. Henry's law coefficients relevant to the biotransformation of thermoplastic starch wastes were developed from Oh and Martin [15, 33]. Table 2 shows the stoichiometric foundations, their chemical equilibrium constants, and the mathematical relationships governed by Eq. (1).

<TABLE 2> Phase equilibria of the biotransformation of maltose [35-40].

2.2.2 Dissociation equilibrium

The carbonates and ammonia, which were highly dissociated and structured with other ionic chemical species in the liquid phase, were strongly dependent on the equilibrium concentration

of protons [H^+]; pH value. The ionic structure of carbonates (CO_3^{-2} and HCO_3^-) was linked to the structure of ammonium ion through the ammonium carbonates: $(NH_4)HCO_3$ and $(NH_4)_2CO_3$. The ionic structures of nitrite (NO_2^-) and nitrate (NO_3^-) were also linked to the ionic structure of ammonium ion through ammonium nitrate (NH_4NO_3). The structure of volatile fatty acids was also linked in the same manner analogous to ammonium formate and ammonium acetate. Thus, an overall ionic cage was established in the liquid phase of the two-phase, batch digester.

$$v_i \mu_i = v_j \mu_j^+ + v_k \mu_k^- \quad (3)$$

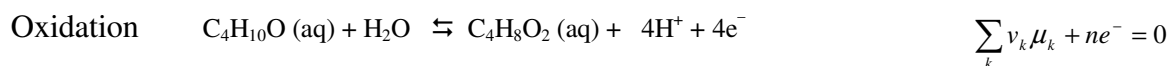
$$K_a = \exp \left\{ \frac{v_i \mu_i^\circ - v_j \mu_j^{\circ+} - v_k \mu_k^{\circ-}}{RT} \right\} = \frac{(a_j^+)^{v_j} (a_k^-)^{v_k}}{a_i^{v_i}} \quad (4)$$

Substituting Eq. (2) into Eq. (3) yielded the ionisation relationship, where equilibrium constants corresponded to dissociation constants (K_a) in the biotransformation of maltose. Table 3 shows the stoichiometric foundations, the chemical equilibrium constants, and the mathematic relationships based on Eq. (4).

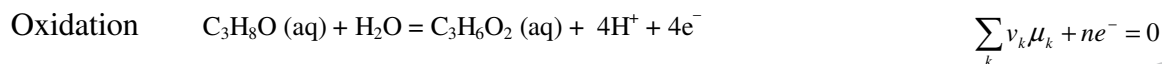
<TABLE 3> Dissociation equilibria of the biotransformation of maltose [35, 37, 38].

2.2.3 Redox equilibrium

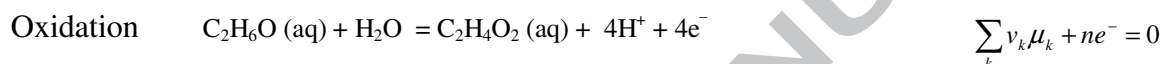
Redox equilibrium is described as a form of coupled half reactions, which never occur by themselves, but that can occur once the electron released by one reactant is accepted by another. Here, the reduction and oxidation potentials were assumed to reach rapidly to a state of equilibrium in the biotransformation of maltose. The half reactions and equilibrium relationships relevant to *acetoclastic bacteria* and *syntrophic acetogenic bacteria* had been developed in the work of Oh and Martin [12, 32, 33]. The half reactions and equilibrium relationships relevant to *fermentative bacteria*, and *anaerobic ammonium oxidising bacteria* had also been developed in the work of Oh and Martin [14], and they were used here without modification. In particular, half reactions and equilibrium relationships relevant to *fermentative bacteria* and *acidogenic bacteria* were developed in this work. An example of *acidogenic bacteria* is given by:



Leading to the overall redox reaction,



Leading to the overall redox reaction,



Leading to the overall redox reaction,



where the pair of half reactions should be in a state of equilibrium, the equilibrium relation being defined by the equality of the pairs of the electrochemical potentials $E(V)$.

$$\sum v_i \mu_i = nFE_i(V) \quad (5)$$

where, F is Faraday's constant, and n is the numbers of electrons transferred. The relationship between the chemical activity (a_i) and electrochemical potential $E(V)$ for the i th half reaction is shown in Eq. (6):

$$nFE_i = \sum v_i \mu_i^\circ + RT \sum v_i \ln a_i \quad (6)$$

Thus, the redox equilibrium is established by the equality of electrochemical potentials:

$$E_i = E_j = E_k = E_l = \dots \quad (7)$$

This electrochemical equilibrium relationship (Eq. 7) allows the exchange of energy between functional microorganisms. This represents a (i) fermentative stage producing an amount of

energy, transferring it into an (ii) acidogenic stage consuming it. Table 4 shows the half reactions representing microbial reactions of the biotransformation of maltose.

<TABLE 4> Redox equilibria of the biotransformation of maltose [35].

2.3 Relationship of activity and fugacity with concentration and partial pressure

2.3.1 Liquid phase

Activity a_i and observable concentration m_i are related by an activity coefficient γ_i [41]. In a non-diluted solution of maltose (ionic activity $>5 \times 10^{-4}$), there are three types of model for the description of the activity coefficients, which can be considered to be the Ideal model, Debye-Hückel model, and Pitzer model. These models are equivalent to the conventional equations of state used to quantify the analogous relationships in the gas phase, and have limited ranges of applicability related to the ionic strength of the liquid phase. These limitations together with their respective models for activity coefficients have been discussed in the work of Oh and Martin [14, 33]. This work reuses their parameter values.

$$a_i = \gamma_i m_i \quad (8)$$

2.3.2 Gas phase

Fugacity (f_i) was related to observable partial pressure ($y_i P$) in an analogous manner to activity and concentration in the liquid phase through a fugacity coefficient (Φ_i):

$$f_i = \Phi_i y_i P \quad (9)$$

where, Φ_i can be derived from a suitable equation of state (EoS). Oh and Martin [33] used Nakamura *et al.*'s EoS to describe the mixture of non-polar and polar gases found in the AD process [39]. This work used the same EoS, thus ensuring consistency between the results.

2.4 Overall phase and mass balances

The equilibrium model requires a strict mass balance condition. The components of overall balances are constituted for the i) gas phase, ii) solute, and iii) pure water from the stoichiometric model.

$$N \sum_i y_i M_{w_i} + \frac{\text{Re}(W)}{55.494} \sum_{i \neq \text{H}_2\text{O}} m_i M_{w_i} + 18.02 \text{Re}(W) = 1000 \text{ (g)} \quad (10)$$

where, N is the total mole of the gas phase, M_{w_i} is the molecular weight of chemical species i , and $\text{Re}(W)$ is the mole numbers of water in solution, in which the total mass of system is conserved to one kg. Strict element material balances: carbon, hydrogen, oxygen, and nitrogen, are also considered. The gas, liquid, and charge balances are considered,

$$\sum_i y_i = 1, \quad \sum_i x_i = 1, \quad \text{and} \quad \sum_i z_i m_i = \text{zero} \quad (11)$$

where, x_i and y_i are the mole-fractions of the i^{th} component in the liquid (x) and gas phase (y), respectively, and z_i is the charge number of the i^{th} component in the liquid phase.

3. RESULTS AND DISCUSSION

The model compound of thermoplastic starch wastes was a maltose. The maltose fed was almost completely hydrolysed and fermented into intermediates, which were further decomposed to carboxylic acids (i.e. VFAs) and carbonates. The residual intermediates: primary alcohols (methanol, ethanol, propanols, glycerol, and butanol), acetaldehyde, acetone, VFAs, and carbon dioxide, remained in the liquid phase. They obeyed Henry's law, and were vaporised into the gas phase. Here, a biotransformation of maltose was electrochemically studied, as the initial mole of maltose was increased in the feedstock at 1 atm and 298.15 K.

3.1 Maltose feedstock in isobaric and isothermal condition

The initial mole of maltose was increased in the feedstock from 0.05 mole kg^{-1} , where the digester became a two-phase (gas/liquid), up to 2.85 mole kg^{-1} , where the water content became almost zero in the initial feedstock. Figure 1 (a) shows two plots of the total number of moles in the gas phase and the liquid phase at 1 atm and 298.15 K. In the same range of initial moles in the maltose feedstock, the gas phase almost linearly expanded as the liquid phase linearly reduced. The result implies that no inhibition was observed in 1 kg of the maltose feedstock, and the initial mole of maltose could be maximised in the feedstock within the operating constraints, such as pumpability. However, Weusthuis *et al.* [42] observed that a biomass yield (grams of

cells/grams of sugar) decreased linearly with increasing amount of the initial mole of maltose in the feedstock. This was attributed to the water activity in the maintenance of living cell.

< **FIGURE 1** >

As the maltose fed was almost completely hydrolysed and fermented into intermediates in the liquid phase, the hydrolytic fermentative stage produced a maximum amount of thermal energy, whilst the acidogenic stage (including acetogenic and acetoclastic processes) consumed a proportional amount of the thermal energy. Figure 1 (b) shows the residual thermal energy (ΔH) linearly decreased from approximately $(-30$ to $-762)$ kJ kg^{-1} as the initial mole of maltose was increased in the feedstock. The residual thermal energy shows a symmetrical relationship to the total number of moles in the gas phase shown in figure 1 (a). These results indicate that the microbial activity of the hydrolytic fermentative stage linearly increased together with the increased microbial activity of the acidogenic stage, but the microbial activity of the hydrolytic fermentative stage was always much greater than the subsequent microbial activities. Thus, it was found that the microbial activity of the hydrolytic fermentative stage showed a constant relationship to the initial mole of maltose fed. The enthalpy analysis was consistent with the overall water balance between the initial water in the maltose feedstock, and the residual water in the equilibrium state. The hydrolytic fermentative stage produced almost a maximum amount of water balance, while as in the manner of the enthalpy analysis, the acidogenic stage (including the acetogenic and acetoclastic processes) consumed a proportional amount of the water. Thus, the residual water was able to represent a relationship between the two microbial stages. Figure 1 (b) shows that as the initial mole of maltose increased in the feedstock, the water balance linearly increased from almost (zero to $+4.93$) mole kg^{-1} . The results indicate that the microbial activity of the hydrolytic fermentative stage ensured that the overall exothermic process was driven to release as much amount of thermal energy to proceed in a forward direction as the gas phase was linearly expanded. In entropy analysis, ΔS showed the same tendency as the change in ΔH at the state of equilibrium ($\Delta G = \text{zero}$). Figure 1 (b) also shows that the biotransformation of maltose constantly exhibited negative, small values of ΔS , which linearly decreased as the initial mole of maltose was increased in the feedstock. This confirms that the microbial activity of the hydrolytic fermentative stage requires a robust microbial activity of acidogenic stage with regard to the bio-catalysts.

Figure 1 (a) shows that as the total number of moles in the gas phase was steadily increased, the mole-fraction of carbon dioxide (CO_2) was not only constant between approximately (0.96 and 0.98) mole mole⁻¹, but the mole-fraction of water was also constant between approximately (0.03 and 0.04) mole mole⁻¹ in the whole range of the initial mole of maltose in the feedstock. This represents that as the initial mole of maltose increased in the feedstock, the microbial activity of acetoclastic process was strongly increased *ad hoc*, and the carbonates produced were increased. Once the carbonates in the liquid phase approached a state of equilibrium, they were mostly in the form of carbonic acid (H_2CO_3), and inhibited the acetoclastic process (c.f. product inhibition), and accumulated acetate. As the carbonic acid was transformed into water and carbon dioxide, and vaporised into the gas phase, the equilibrium concentration of acetate was steadily decreased, and further degraded to carbonates. Figure 2 shows the production of mole of acetate in the initial mole of maltose fed. The range $10^{-2} < x < 1$ shows that as the initial mole fraction of maltose was increased, the equilibrium acetic acid fraction steadily decreased, as already explained. The low range, $10^{-3} < x < 10^{-2}$ shows that the equilibrium acetic acid fraction was strongly dependent on low initial concentrations of maltose, and that as this concentration was increased, the dependence became stronger. The 'rapid transition' in the range $10^{-4} < x < 10^{-3}$, was attributable to the rapid phase transition that occurred as carbonates were vaporised into the gas phase. The empirical observations made by Yu *et al.* [43] in the up-flow batch digestion of lactose with initial 40 g l⁻¹ COD of lactose show reasonable agreement with the thermodynamic equilibrium, suggesting that the process achieved a good approach to equilibrium throughout the digestion period. As the initial lactose concentration was increased, the phase of digester was changed from single-phase in the range $10^{-4} < x < 10^{-3}$, to two-phase, but ammonium ions were prevented by the vaporisation of carbonates. Despite this, the underlying trend agreed with that predicted by the equilibrium model. The empirical observations made by Lu *et al.* [44] in a batch digestion of Cassava digestion show qualitative agreement with the equilibrium model. Interestingly, the agreement is best at higher initial maltose concentration. The empirical observations made by Puranjan *et al.* [45] in a batch digestion of palm oil waste, also show good agreement with the equilibrium model. Together, these empirical observations of biotransformation suggest that in the digestion of maltose, the observed inhibition of the acetogenic and acetoclastic processes is attributable in part to the overall thermodynamic origins, rather than exclusively to bio-kinetic sources.

< **FIGURE 2** > [43-45].

In the liquid phase, the intermediates show very small values in magnitude throughout the whole range of the initial mole of maltose in the feedstock, but the VFAs (caproic, valeric, butyric, propionic, acetic, and formic acids) show in the highest concentrations at 1 atm and 298.15 K. Figure 1 (c) shows that as the water activity decreases, the total mole-fraction of VFAs symmetrically increases. At 2.85 mole kg⁻¹ of maltose feedstock, the total mole-fraction of VFAs finally corresponded to the water activity (approximately 0.5:0.5). It was found that the mole-fractions of valerate, butyrate, and propionate logarithmically increased, while the mole-fraction of acetate showed almost flat, describing a parabola in the whole range of the initial mole of maltose as shown in figure 1 (d), where the maximum concentrations of acetate, propionate, and butyrate were observed to be (9.12, 0.71, and 22.8) g l⁻¹ respectively. The model supported the empirical observation of Zheng and Yu [46] that overall bioactivity was acutely reduced by 50 % in a dark fermentation when the concentration of butyrate reached 20.78 g l⁻¹. The equilibrium of acetate describing a parabola has already been explained in the previous section. As the gas phase was increased, the degradation of acetate steadily increased, but produced a large amount of protons. Figure 3 (a) shows that as the initial mole fraction of maltose was increased, the pH value was steadily decreased, and then became almost constant (\approx pH 3.0). This readily reached a state of equilibrium in protons, and inhibited the acetogenic process of converting VFAs to acetate. The result shows good agreement with the empirical work of Ezeji, Qureshi *et al.* [47] that had shown a product-inhibition at 8.5 g l⁻¹ of acetate in ABE fermentation.

< **FIGURE 3** > [43-45].

Figure 3 (b) shows that the proportional value (NAD⁺/NADH) steadily increased from approximately 10⁻⁴ to 0.01. This simply means that NADH was converted (oxidised) into NAD⁺, releasing electrons and protons to support the microbial activity of the first hydrolytic fermentative stage, although the oxidised NAD⁺ showed very small values (<10⁻⁵). From a microbial point of view, it indicates that the second acidogenic stage, including the acetogenic and acetoclastic processes, was much stronger than the first hydrolytic fermentative stage. It also provides evidence supporting the thesis that the CAC produced a little ATP energy in the whole range of the initial mole of maltose. Interestingly, the evidence was consistent with the acetoclastic process being steadily increased as the gas phase increased. The proportions of NAD⁺/NADH also allowed calculation of the equilibrium of electrochemical potentials ψ , and the potential values indicated a stage of electron-transference amongst the individual microbial

stages. Figure 3 (b) shows that the overall process was simply oxidised on increasing the initial mole of maltose in the feedstock, and the required electron donors, such as acetate.

Consequently, there was no thermodynamic inhibition observable in the first hydrolytic fermentative stage, while there were strong thermodynamic inhibitions in the second acidogenic stage. In particular, the acetoclastic process followed by the acetate accumulation was observed, and almost no ATP generation was observable in the state of equilibrium of single-phase fermentation. The strong inhibition was steadily decreased by the vaporisation of carbonic acid, while the secondary inhibition was also observed in the two-phase digester. In the presence of the acidogenic stage, the acetogenic process, which was particularly inhibited, accumulated the VFAs. These results provided a clue of how to overcome the thermodynamic inhibitions in the biotransformation of maltose. A vaporisation of carbonates, such as a depressurised digester, is able to overcome the inhibition of accumulated acetate, and fixation of the proton concentration by a buffer solution is also able to prevent an inhibition of acetogenic process in the biotransformation of maltose. However, the fixation of pH value may significantly reduce the natural performance of the microbial kinetics with the microbial association sharing their metabolites. In the next section, the authors focus on an operation parameter, pressure, in the biotransformation of maltose.

3.2 Depressurised digester in isothermal condition

The digester was depressurised from one to 3×10^{-4} atm where the residual water vanished in the liquid phase (approximately residual $\text{H}_2\text{O} \approx 1 \times 10^{-6}$ mole kg^{-1}). Figure 4 (a) shows that as the digester was depressurised, the decrease in the total number of moles in the liquid phase was compensated by the total number of moles in the gas phase. When the pressure reached around the saturated vapour pressure of water (about 2×10^{-2} atm), water molecules were mostly vaporised into the gas phase, and became in a quasi-state of azeotrope condition (at about 4×10^{-2} atm), where the total number of moles in the liquid phase was equivalent to the total number of moles in the gas phase. As the pressure hypothetically decreased, the total number of moles in the liquid phase continued to decline, and then almost vanished, but the total number of moles in the gas phase steeply increased. This simply means that when the pressure was slightly reduced, it did not influence the fermentation, while as the pressure was severely decreased in the mid-range of pressure ($2 \times 10^{-2} < P, \text{ atm} < 0.1$), the residual water only vaporised, and then volatile

compounds were vaporised in the hypothetical range of pressure ($P, \text{atm} < 2 \times 10^{-2}$). The details of mole-fractions in the gas phase were further investigated.

< **FIGURE 4** >

Figure 4 (b) shows that as the digester was depressurised from one atm, the mole-fraction of water ($y_{\text{H}_2\text{O}}$) in the gas phase exponentially increased, and reached 0.71 at about 2×10^{-2} atm, whilst the mole-fraction of carbon dioxide (y_{CO_2}) symmetrically decreased from 0.98 at 1 atm to 0.22 at approximately 2×10^{-2} atm. As a result of the model showing good agreement with Raoult's law in the same region of the depressurised digester ($2 \times 10^{-2} < P, \text{atm} < 1.0$), the constant water activity ($x_{\text{H}_2\text{O}}=0.83$) in the liquid phase dramatically decreased down to 0.5 at 2×10^{-2} atm, as shown in figure 4 (c). Figure 4 (b) shows that as the pressure was further decreased, the $y_{\text{H}_2\text{O}}$ inversely reduced from 0.71 (at 2×10^{-2} atm) to 0.55 (at 5×10^{-3} atm), and then steadily dropped to 0.3. This means that the water vaporisation was almost completed in the mass conservation of 1 kg, and the depressurised digester suddenly produced $\text{C}_2\text{H}_6\text{O}$ (acetone) and H_2 in the hypothetical range of pressure ($3 \times 10^{-4} < P, \text{atm} < 2 \times 10^{-2}$). As hydrogen (H_2) and acetone appeared from 5×10^{-2} atm, the mole-fractions increased up to 0.33 and 0.13 at 5×10^{-3} atm respectively. The results show good agreement with the empirical observation of Kisielewska *et al.* [48] that a depressurised fermentation was more effective in enhancing bio-hydrogen production than dark fermentative hydrogen production at atmospheric pressure. This tells us that the whole depressurised digester relies on the extent of water contents in the system. As the pressure approaches the saturated vapor pressure of water, the overall system degrades the accumulated VFAs and produces hydrogen. The hydrogen reacts with the existing shorter chain alcohols (methanol, ethanol and propanols) and is converted to acetone.

< **FIGURE 5** >

In the liquid phase, the intermediates had very low concentrations in the whole range of depressurised fermentation, while the volatile fatty acids observed had the largest concentrations in the liquid phase. Figure 4 (c) shows that the total mole-fraction of VFAs was in steady state, and was almost constant (≈ 0.16) in the mid-range of pressure ($0.1 < P, \text{atm} < 1.0$), while as the pressure reached the approximate saturated vapour pressure of water, the total mole-fraction symmetrically increased from 0.16 (at 5×10^{-2} atm) to 0.5 (at 2×10^{-2} atm). This resulted from the massive vaporisation of water based on Raoult's law, which has already been explained in the

previous section. In the same region of pressure, figure 4 (d) shows that individual mole-fractions of VFAs (butyrate, propionate and acetate) decreased. This resulted from the decrease in the mole-fraction of carbonate. This effect will be explained in the next section. Interestingly, it can be seen that the humps in the mole-fractions of valerate and butyrate are attributable to the massive water vaporisation in the low range of pressure ($2 \times 10^{-2} < P, \text{ atm} < 0.1$), so the result shows that the acetogenic process was inhibited, and accumulated valerate and butyrate as the pressure decreased. The results were similar to the empirical observation of Ezeji *et al.* [47] that gas stripping with CO_2 and H_2 in low range pressure incurred an unusually high concentration of VFAs in the fermentation.

As the pressure was hypothetically decreased, figure 4 (c) also shows the water activity dramatically decreased from 0.5 (at 2×10^{-2} atm) to almost zero (at 3×10^{-4} atm). However, the mole-fraction of VFAs inversely decreased, and then become nearly zero (at 3×10^{-4} atm). This means that the microbial activity of the acidogenic stage was entirely inhibited, and the VFAs completely vanished. Here, the overall mass balance shown in figure 5 (a) means that as the acidogenic stage, including acetogenic and acetoclastic processes, was entirely inhibited, a production of mixture (acetone, butanol and CO_2) was thermodynamically observed in the low range of pressure, and then the acetone and butanol were further degraded into carbonates, together with water reduction, in the hypothetic range of pressure.

Figure 4 (e) shows that although the pressure was decreased to the vapour pressure of water (2×10^{-2} atm), the pH values had almost constant values (\approx between pH (3.2 and 3.1)) in the mid and low range of pressure ($2 \times 10^{-2} < P, \text{ atm} < 1$). This contrasts with the mole-fraction of VFAs shown in figure 4 (c), which resulted from the presence and accumulation of ammonium ions. As the pressure hypothetically continued to decrease from 2×10^{-2} atm, the pH values suddenly stepped up to 4.3 (at 5×10^{-3} atm), and then steadily increased to pH 5 (at 3×10^{-4} atm). The result was consistent with the mole fraction of VFAs that was vanished and converted into butanol and acetone, as shown in figure 5 (a).

Figure 4 (f) shows that as the digester was depressurised from one to 2×10^{-2} atm, the ΔH slightly increased from about -548 kJ kg^{-1} (at 1 atm) to -440 kJ kg^{-1} (at 5×10^{-2} atm), and then steeply increased up to $+500 \text{ kJ kg}^{-1}$ at 2×10^{-2} atm (the saturated vapour pressure of water). The enthalpy change ($+940 \text{ kJ kg}^{-1}$) between (5×10^{-2} and 2×10^{-2}) atm corresponds to around 20.0

moles of water vaporised, and this is approximately equivalent to the total number of moles that transferred from the liquid phase into the gas phase (figure 4 (a)). The ΔH was again rapidly increased to $+930 \text{ kJ kg}^{-1}$ at $5 \times 10^{-3} \text{ atm}$, and then it became steadily increased to $+1,190 \text{ kJ kg}^{-1}$ (at $3 \times 10^{-4} \text{ atm}$). The results imply that the biotransformation of maltose requires an amount of thermal energy in terms of ATP energy, and the entirely carbonaceous feedstock was converted into acetone through butanol. An inhibition of the acidogenic stage, including the acetogenic and acetoclastic processes, was observed around the saturated vapour pressure of water, while the microbial activity dramatically produced butanol and acetone. However, the water balance was steadily increased from $+3.3 \text{ mole kg}^{-1}$ (1 atm) to $+3.45 \text{ mole kg}^{-1}$ (at $4 \times 10^{-2} \text{ atm}$) and then steeply dropped to $-4.6 \text{ mole kg}^{-1}$ (at $3 \times 10^{-4} \text{ atm}$). This means that the overall acidogenic stage was not inhibited, but VFAs were completely converted into acetone through butanol. Figure 4 (f) also shows that the entropy change (ΔS) corresponded to the number of moles in the gas phase shown in figure 4 (a). Interestingly, the ΔS became zero (at $P = 4 \times 10^{-2} \text{ atm}$), before the pressure reached the saturated vapour pressure of water (approximately $2 \times 10^{-2} \text{ atm}$). This means that the hydrolytic fermentation and the sequent degradation of the fermented products were thermodynamically spontaneous, as long as an amount of thermal energy ($> +1,190 \text{ kJ kg}^{-1}$) was provided, but the subsequent vaporisation of water only influenced the change of entropy and enthalpy.

Consequently, the depressurised digester is entirely dependent on water contents in the two-phase system. As the pressure approaches the saturated vapour pressure of water, the overall system directly converts the accumulated short chain VFAs to acetone and then produces hydrogen and carbon dioxide. The produced hydrogen increases the partial pressure, while also reacts with the existing shorter chain alcohols (methanol, ethanol and propanols) and converts them to acetone at a starvation of mono and or di-saccharides. The reaction is successively iterated (in clock-wise) and the product (acetone) is highly vaporised and stored into the gas phase, when carbonates have very small quantities in the liquid phase or when the 'citric acid cycle' decreases. Secondly existing longer chain fatty acids are constantly degraded to the shorter chain fatty acids but the butyrate is directly converted to butanols, which are again converted into the shorter chain alcohols (methanol, ethanol, and propanols) and following the former pathway (in anti-clock-wise). Figure 6 shows the reaction coordinates with the relative enthalpy change. The new metabolic pathway that was thermodynamically proved can be applied in the starvation

of mono and or di-saccharides at extreme conditions, and it is significantly different from the conventional pathway through ‘acetoacetate’. In particular, it is peculiar that a minimisation of the ATP production in the iteration of CAC and that the long chain VFAs are utilized and converted to acetone through butanol for the purpose of constant maintenance of cells.

< FIGURE 6 >

3.3 Pressurised digester in isothermal condition

Pressure dependence was investigated in isothermal condition (298.15 K). Two moles of maltose were injected into 17.2 moles of H₂O, and a total 1 kg of strict mass was then conserved in a two-phase digester. The absolute pressure was increased from (one up to 100) atm in which range micro-bioreactors [34] usually operate. Figures 4 (a) and (b) show that as the digester was pressurised, a few moles of carbon dioxide in the gas phase were transferred into the liquid phase and the solubility of carbonates increased. Figure 4 (c) show that as the solubility of carbonates ($x\text{CO}_2$) steadily increased, the water activity ($x\text{H}_2\text{O}$) symmetrically decreased from 0.83 (at 1 atm) to 0.73 (at 100 atm), whereas figure 4 (b) further shows that water ($y\text{H}_2\text{O}$) and carbon dioxide ($y\text{CO}_2$) were almost constant values in the gas phase in the same region of pressures. The results tell that as the pressure increased, the gas phase decreased and then the digester reached at the phase equilibrium, in which acetate accumulation occurred. This work agreed with the work of Oh and Martin [12, 14, 15, 32, 33], in that the acetoclastic process that obeyed Le Chatelier’s principle was inhibited in high carbon dioxide solubility. The acetoclastic inhibition has already been explained in the previous section.

As the digester was pressurised from one to 100 atm, figure 4 (f) shows that the change of enthalpy (ΔH) was steadily decreased from approximately -548 kJ kg^{-1} (at 1 atm) to -644 kJ kg^{-1} (at 100 atm). This showed the same feature of the total number of moles in the gas phase, as shown in figure 4 (a), which means that the carbon dioxide in the gas phase was condensed. Figure 4 (f) also shows that the water balance was steadily decreased from $+3.3 \text{ mole kg}^{-1}$ (at 1 atm) to $+1.5 \text{ mole kg}^{-1}$ (at 100 atm), while figure 4 (e) shows that the pH value steadily decreased from approximately pH 3.2 (at 1 atm) to almost constant value (\approx pH 3.0 at 100 atm). Thus, these results confirm that the acetogenic process continued to decompose the VFAs into acetate in the high-pressure condition. Figure 4 (d) also shows that the individual mole-fractions of VFAs in the liquid phase were increased together with the mole-fraction of carbonates

throughout the whole region of pressure. However, the mole-fraction of valerate was only steadily decreased. Figure 5 (a) also shows that the total weight of carbonates was constant throughout the whole range of pressurised digester. These results imply that in the presence of strong acetoclastic inhibition, valerate only degraded into acetate, which accumulated in the high range of pressure. The result also showed qualitative agreement with the work of Chen *et al.* [49] that reported an accumulation of acetic acid with short chain fatty acids in batch pectic-oligosaccharides fermentation at 155 MPa.

4. CONCLUSION

From the results of the biotransformation of thermoplastic starch wastes, it was found that the organic wastes were initially fermented in a single-phase (i.e. liquid phase), which was strongly governed by microbial kinetic behaviour. The fermentation excreted acetate, so as to utilise residual energy. As the carbonates produced were vaporised, it was found that the two-phase digestion generated an amount of energy from the decomposition of the accumulated acetate, while the acetoclastic process was regulated by the vaporisation of carbon dioxide. The result clearly tells us that the glycolysis did not coincide together with the citric acid cycle in the batch fermentation. Herein, the pressurized digester inhibited significantly the acetoclastic process and decomposed valerate successively while the glycolysis was able to coincide together with the citric acid cycle in the two-phase, pressurised fermentation. Interestingly, the depressurised digester completely converted the accumulated VFAs into acetone and alcohols (mainly butanols) around the saturated vapour pressure of water. The new catabolism rapidly transforms the short-chain fatty acids (acetate, propionate, and butyrate) to alcohols and then the residual alcohols are stored as acetone. The new metabolic pathway thermodynamically proved, is involved the conventional pathway through ‘acetoacetate’ and the study can be also applied to a cell metabolism and or microbial diversity in extreme conditions such as the starvation of saccharides.

REFERENCES

- [1] Plastics-Europe, Plastics - an analysis of European plastics production, demand and waste data the Facts 2016, PlasticsEurope, 2016.
- [2] Jenna R. Jambeck, Roland Geyer, Chris Wilcox, Theodore R. Siegler, Miriam Perryman, Anthony Andrady, Ramani Narayan, Kara Lavender Law, Plastic waste inputs from land into the ocean, *Science* 347 (2015) pp. 768-771.
- [3] DEFRA, The UK statistics on waste, in: DEFRA (Ed.), DEFRA, 2016.
- [4] US. EPA, Advancing Sustainable Materials Management: 2013 Fact Sheet, in: U.E.P. Agency (Ed.), EPA, Washington, DC 20460, 2015.
- [5] Karl West, Waste not, want not: how the rubbish industry learned to look beyond landfill, *The guardian*, 2015.
- [6] HM-Revenue and Customs, Rates and allowances: HM Revenue and Customs: Environmental taxes, reliefs and schemes for businesses, in: H.R.a. Customs (Ed.), 2017.
- [7] Bruce Watson, Can incineration and landfills save us from the recycling crisis?, *The Guardian*, *The Guardian*, 2016.
- [8] ISO, Anaerobic biodegradability in plastics, in: ISO (Ed.) ISO 15985:2014, ISO, 2014.
- [9] Marco Capodici, Santo Fabio Corsino, Francesca Di Pippo, Daniele Di Trapani, Michele Torregrossa, An innovative respirometric method to assess the autotrophic active fraction: Application to an alternate oxic–anoxic MBR pilot plant, *Chemical Engineering Journal* 300 (2016) pp 367-375.
- [10] Jason J. Plumb, Joanne Bell, David C. Stuckey, Microbial Populations Associated with Treatment of an Industrial Dye Effluent in an Anaerobic Baffled Reactor, *Appl. Environ. Microbiol.* 67 (2001) pp 3226-3235.
- [11] Maureen N. Kinyua, Matthew Elliott, Bernhard Wett, Sudhir Murthy, Kartik Chandran, Charles B. Bott, The role of extracellular polymeric substances on carbon capture in a high rate activated sludge A-stage system, *Chemical Engineering Journal* 322 (2017) pp 428-434.
- [12] S.T. Oh, A.D. Martin, Long chain fatty acids degradation in anaerobic digester: thermodynamic equilibrium consideration, *Process Biochemistry* 45 (2010) pp 335-345.
- [13] L.O. Ingram, Mechanism of lysis of *Escherichia coli* by ethanol and other chaotropic agents, *J. Bactol.* 146 (1981) pp 331-336.
- [14] S.T. Oh, A.D. Martin, Glucose contents in anaerobic ethanol stillage digestion manipulate thermodynamic driving force in between hydrogenophilic and acetoclastic methanogens, *Chemical Engineering Journal* 243 (2014) pp 526-536.
- [15] S.T. Oh, A.D. Martin, Thermodynamic efficiency of carbon capture and utilisation in anaerobic batch digestion process, *Journal of CO2 Utilization* 16 (2016) pp 182–193.
- [16] Maureen N. Kinyua, Mark W. Miller, Bernhard Wett, Sudhir Murthy, Kartik Chandran, Charles B. Bott, Polyhydroxyalkanoates, triacylglycerides and glycogen in a high rate activated sludge A-stage system, *Chemical Engineering Journal* 316 (2017) 350-360.
- [17] Sabrina Campanari, Floriana Augelletti, Simona Rossetti, Fabio Sciubba, Marianna Villano, Mauro Majone, Enhancing a multi-stage process for olive oil mill wastewater valorization towards polyhydroxyalkanoates and biogas production, *Chemical Engineering Journal* 317 (2017) pp 280-289.
- [18] Joana M.B. Domingos, Salvatore Puccio, Gonzalo A. Martinez, Natacha Amaral, Maria A.M. Reis, Serena Bandini, Fabio Fava, Lorenzo Bertin, Cheese whey integrated valorisation: Production, concentration and exploitation of carboxylic acids for the production of polyhydroxyalkanoates by a fed-batch culture, *Chemical Engineering Journal* 336 (2018) pp 47-53.

- [19] M. Russo, C. O'Sullivan, B. Rounsefell, P.J. Halley, R. Truss, W.P. Clarke, The anaerobic degradability of thermoplastic starch: Polyvinyl alcohol blends: Potential biodegradable food packaging materials, *Bioresource Technology* 100 (2009) pp 1705-1710.
- [20] S.J. Liu, A. Steinbüchel, Exploitation of butyrate kinase and phosphotransbutyrylase from *Clostridium acetobutylicum* for the in vitro biosynthesis of poly(hydroxyalkanoic acid), *Applied Microbiology and Biotechnology* 53 (2000) pp 545-552.
- [21] Shuang-Jiang Liu, Alexander Steinbüchel, A Novel Genetically Engineered Pathway for Synthesis of Poly(Hydroxyalkanoic Acids) in *Escherichia coli*, *Appl. Environ. Microbiol.* 66 (2000) pp. 739-743.
- [22] Di Cai, Zhen Chang, Lili Gao, Changjing Chen, Yuanpu Niu, Peiyong Qin, Zheng Wang, Tianwei Tan, Acetone-butanol-ethanol (ABE) fermentation integrated with simplified gas stripping using sweet sorghum bagasse as immobilized carrier, *Chemical Engineering Journal* 277 (2015) 176-185.
- [23] Charles ENakamura, Gregory MWhited, Metabolic engineering for the microbial production of 1,3-propanediol *Current Opinion in Biotechnology* 14 (2003) pp 454-459.
- [24] Zhe Wu, Zhe Wang, Guoqing Wang, Tianwei Tan, Improved 1,3-propanediol production by engineering the 2,3-butanediol and formic acid pathways in integrative recombinant *Klebsiella pneumoniae*, *Journal of Biotechnology* 168 (2013) pp 194-200.
- [25] Y. Zhang, T. Hou, B. Li, C. Liu, X. Mu, H. Wang, Acetone-butanol-ethanol production from corn stover pretreated by alkaline twin-screw extrusion pretreatment, *Bioprocess. Biosyst. Eng.* 37 (2014) pp. 913-921.
- [26] B. Ndaba, I. Chiyanzu Marx, n-Butanol derived from biochemical and chemical routes: A review. , *Biotechnology Reports* 8 (2015) pp 1-9.
- [27] Manuel Becerra, María Esperanza Cerdán, María Isabel González-Siso, Biobutanol from cheese whey, *Microbial Cell Factories* 14 (2015) pp 1-14.
- [28] L. Li, H. Ai, S. Zhang, S. Li, Z. Liang, Z. Wua, S. Yang, J. Wang, Enhanced butanol production by coculture of *Clostridium beijerinckii* and *Clostridium tyrobutyricum*, *Bioresour. Technol.* 143 (2013) pp 397-404.
- [29] J. Li, X. Chen, B. Qi, J. Luo, Y. Zhang, Y. Sub, Y. Wan, Efficient production of acetone-butanol-ethanol (ABE) from cassava by a fermentation-pervaporation coupled process, *Bioresour. Technol.* 169 (2014) pp. 251-257.
- [30] Di Cai, Huidong Chen, Changjing Chen, Song Hu, Yong Wang, Zhen Chang, Qi Miao, Peiyong Qin, Zheng Wang, Jianhong Wang, Tianwei Tan, Gas stripping-pervaporation hybrid process for energy-saving product recovery from acetone-butanol-ethanol (ABE) fermentation broth, *Chemical Engineering Journal* 287 (2016) pp 1-10.
- [31] S.T. Oh, A.D. Martin, Loss of thermodynamic spontaneity in methanogenic consortium with ammonal contents, *Chemical engineering journal* 243 (2014) pp 244-253.
- [32] S.T. Oh, A.D. Martin, A thermodynamic equilibrium consideration of the effect of sodium ion in acetoclastic methanogenesis, *J Chem Technol Biotechnol* 88 (2013) pp 834-844.
- [33] S.T. Oh, A.D. Martin, Thermodynamic equilibrium model in anaerobic digestion process, *Biochemical Engineering Journal* 34 (2007) pp 256-266.
- [34] C.M. Nelson, M.R. Schuppenhauer, D.S. Clark, High-pressure, high-temperature bioreactor for comparing effects of hyperbaric and hydrostatic pressure on bacterial growth., *Appl. Environ. Microbiol.* 58 (1992) pp. 1789-1793.
- [35] M. Pourbaix, Atlas of electrochemical equilibria in aqueous solutions, NACE Cebelcon., New York, 1974.
- [36] A.H. Harvey, Semiempirical correlation for Henry's constants over large temperature ranges, *Journal of American Institute Chemical Engineering* 42 (1996) pp 1491-1494.

- [37] Carl. L. Yaws, Chemical properties handbook, 1 ed., McGraw Hill, New York, 1997.
- [38] Carl. L. Yaws, Yaws' handbook of thermodynamic and physical properties of chemical compounds, 2003.
- [39] Ryoji Nakamura, Gerrit J.F. Breedveld, John M. Prausnitz, Thermodynamic properties of gas mixtures containing common polar and nonpolar components, Industrial Engineering Chemical Process Design Division 15 (1976) pp. 557 -564.
- [40] Nakamura R, B. GJF, Prausnitz JM, Thermodynamic Properties of gas mixtures containing common polar and nonpolar components, Ind Eng, Chem Process Design Division 15 (1976) pp 557-564.
- [41] W. Stumm, J.J. Morgan, Aquatic chemistry, John Wiley & Sons, Inc, New York, 1996.
- [42] R.A. Weusthuis, H. Adams, W.A. Scheffers, J.P. van Dijken, Energetics and kinetics of maltose transport in *Saccharomyces cerevisiae*: a continuous culture study., Appl. Environ. Microbiol. 59 (1993) pp 3102-3109.
- [43] H.Q. Yu, Y. Mu, H.H. Fang, Thermodynamic analysis of product formation in mesophilic acidogenesis of lactose, Biotechnology and Bioengineering 87 (2004) pp 813-822.
- [44] C. Lu, J. Zhao, S. Yang, D. Wei, Fed-batch fermentation for n-butanol production from Cassava bagasse hydrolysate in a fibrous bed bioreactor with continuous gas stripping, Bioresour Technol 104 (2012) pp 380-387.
- [45] Puranjan Mishra, Sveta Thakur, Lakhveer Singh, Zularisam Ab Wahid, Mimi Sakinah, Enhanced hydrogen production from palm oil mill effluent using two stage sequential dark and photo fermentation, International Journal of Hydrogen Energy 41 (2016) pp 18431-18440.
- [46] X.J. Zheng, H.Q. Yu, Inhibitory effects of butyrate on biological hydrogen production with mixed anaerobic cultures, Journal of Environmental Management 74 (2005) pp 65-70.
- [47] T.C. Ezeji, N. Qureshi, H.P. Blaschek, Acetone butanol ethanol (ABE) production from concentrated substrate: reduction in substrate inhibition by fed-batch technique and product inhibition by gas stripping, Applied Microbiology and Biotechnology 63 (2004) pp 653-658.
- [48] M. Kisielewska, M. Dębowski, M. Zieliński, Improvement of biohydrogen production using a reduced pressure fermentation, Bioprocess Biosyst Eng. 38 (2015) pp 1925-1933.
- [49] J. Chen, R.H. Liang, W. Liu, T. Li, C.M. Liu, S.S. Wu, Z.J. Wang, Pectic-oligosaccharides prepared by dynamic high-pressure microfluidization and their in vitro fermentation properties, Carbohydr Polym. 91 (2013) pp 175-182.

FIGURE CAPTIONS

FIGURE 1. Biotransformation of maltose versus the initial mole of maltose (at 1atm and 298.15 K); where (A) phase transition, (B) enthalpy change and water production, (C) water activity and VFAs, and (D) individual mole-fractions of VFAs; pressure dependence was studied at the dot line

FIGURE 2. Thermodynamic inhibition of acetate accumulated in biotransformation of maltose (at 1 atm and 298.15 K), where a single-phase was separated into a two-phase at the dot line; ● empirical observation of palm oil waste fermentation [1], ○ empirical observation of lactose fermentation [2] and ◇ empirical observation of Cassava fermentation [3]

FIGURE 3. Biotransformation of maltose versus the initial mole-fraction of maltose (at 1 atm and 298.15 K), where the single-phase was separated into a two-phase at the dot line; (A) pH value and (B) electrochemical potentials and NAD^+/NADH ratio; ● empirical observation of palm oil waste fermentation [1], ○ empirical observation of lactose fermentation [2] and ◇ empirical observation of Cassava fermentation [3]

FIGURE 4. Pressure dependence in biotransformation of maltose with 2 mole kg^{-1} of maltose feedstock at 298.15 K, where a concentration dependence of maltose feedstock was studied at the dot line; (A) phase transition, (B) mole-fraction in the gas phase (C) mole-fraction in liquid phase, (D) individual mole-fractions of VFAs in the liquid phase, (E) pH value and NAD^+/NADH ratio and (F) enthalpy change and water production

FIGURE 5. Pressure dependence in biotransformation of maltose with 2 mole kg^{-1} of maltose feedstock at 298.15 K, where a concentration dependence of maltose feedstock was studied at the dot line; (A) mass balance and (B) electrochemical potential

FIGURE 6. Reactions coordinate of beta-oxidation (catabolism) with energy storage (biosynthesis)) at the starvation of carbohydrates

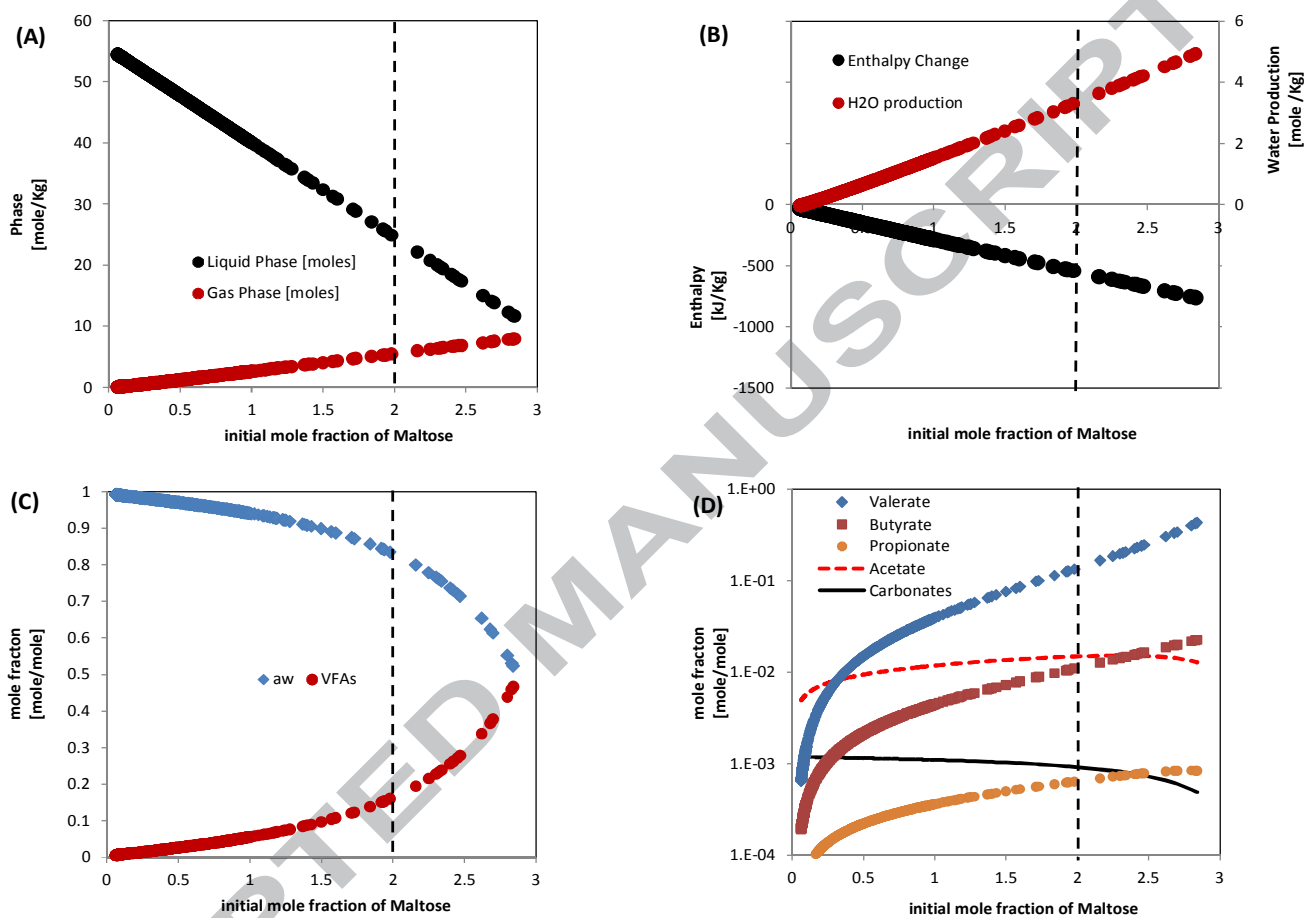


FIGURE 1. Biotransformation of maltose versus the initial mole of maltose (at 1atm and 298.15 K); where (A) phase transition, (B) enthalpy change and water production, (C) water activity and VFAs, and (D) individual mole-fractions of VFAs; pressure dependence was studied at the dot line

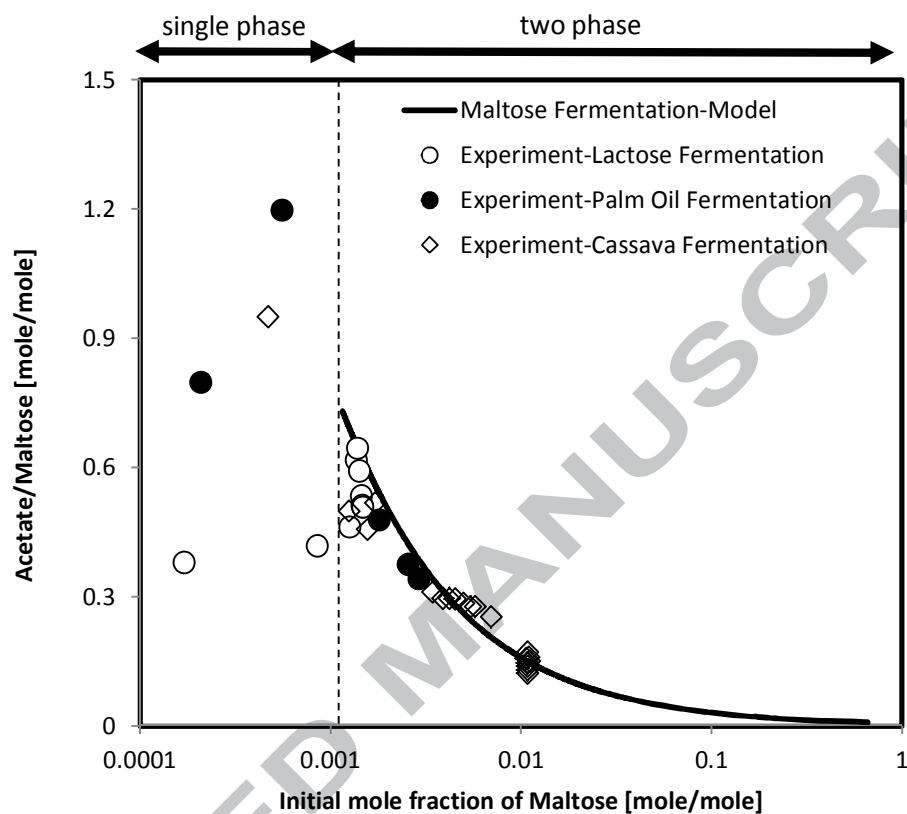


FIGURE 2. Thermodynamic inhibition of acetate accumulated in biotransformation of maltose (at 1 atm and 298.15 K), where a single-phase was separated into a two-phase at the dot line; ● empirical observation of palm oil waste fermentation [1], ○ empirical observation of lactose fermentation [2] and ◇ empirical observation of Cassava fermentation [3]

ACCEPTED MANUSCRIPT

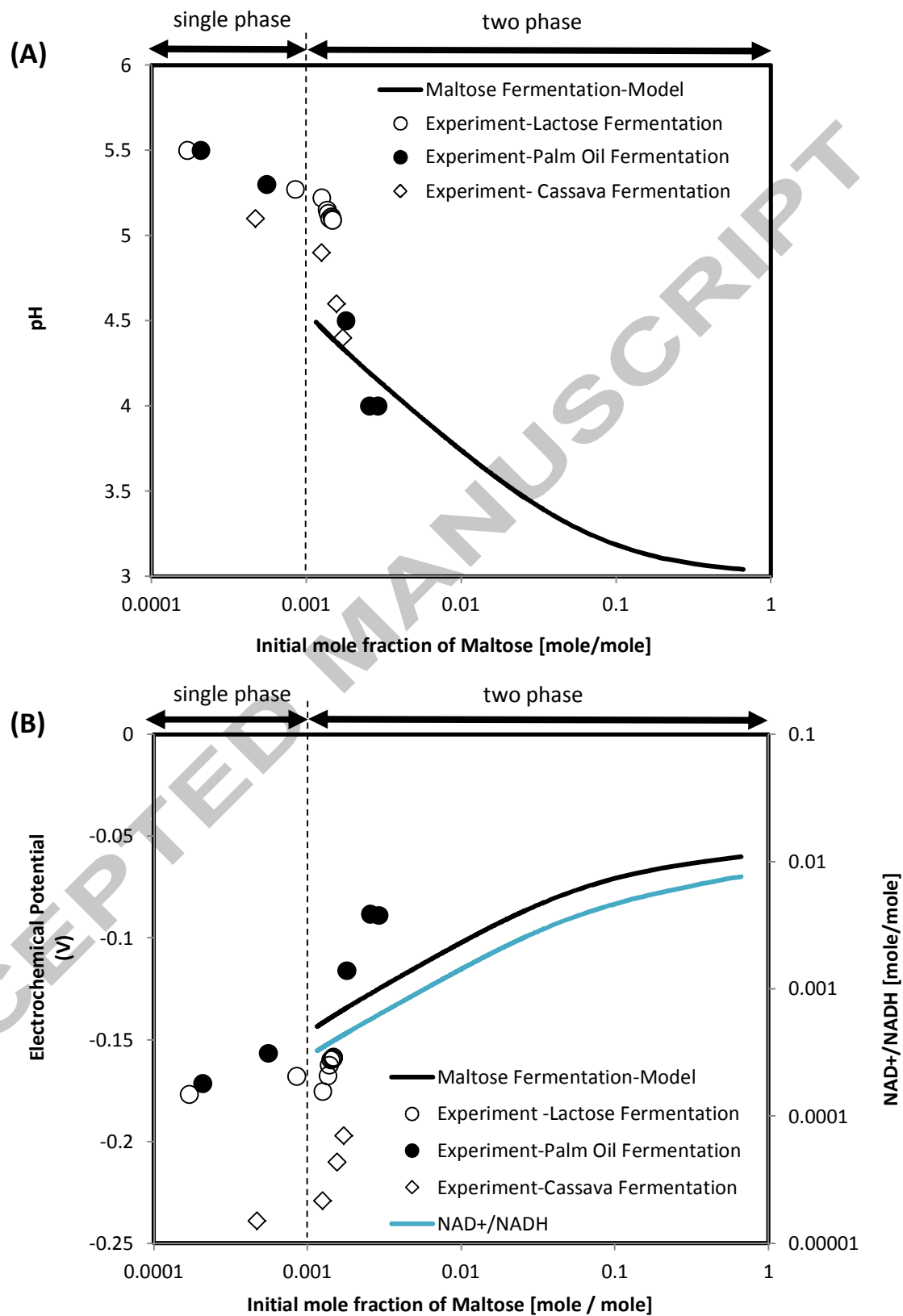


FIGURE 3. Biotransformation of maltose versus the initial mole-fraction of maltose (at 1 atm

and 298.15 K), where the single-phase was separated into a two-phase at the dot line; (A) pH value and (B) electrochemical potentials and NAD^+/NADH ratio; ● empirical observation of palm oil waste fermentation [1], ○ empirical observation of lactose fermentation [2] and ◇ empirical observation of Cassava fermentation [3]

ACCEPTED MANUSCRIPT

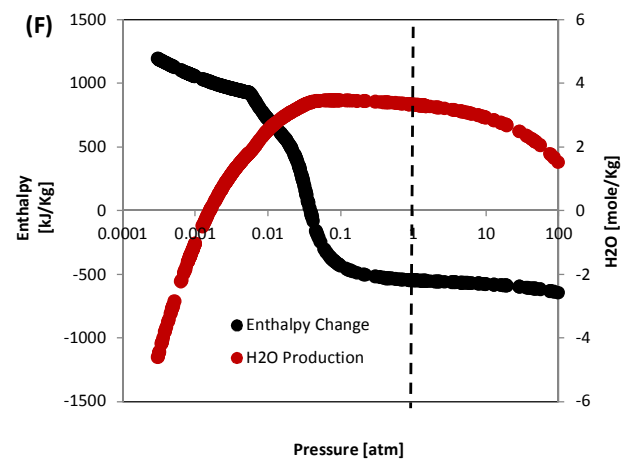
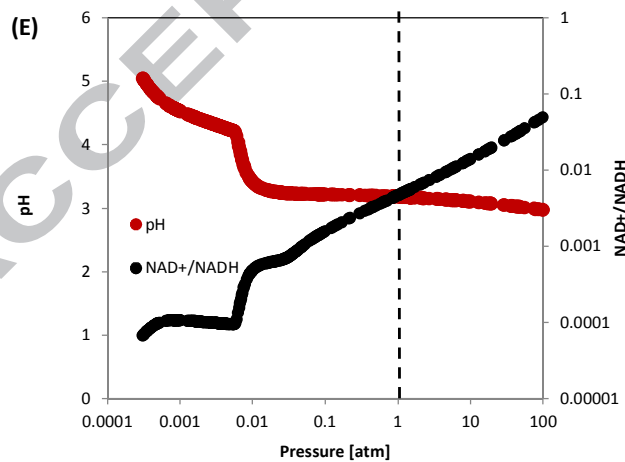
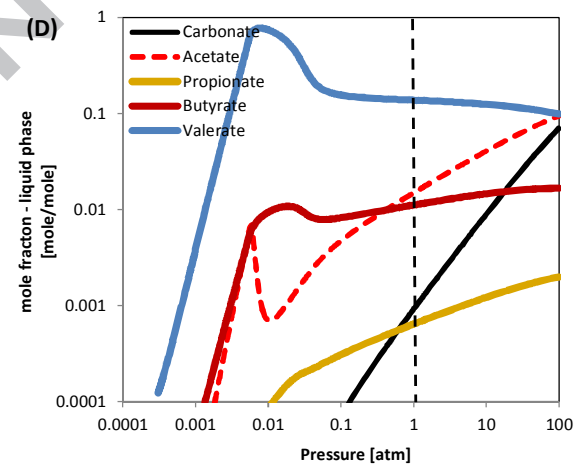
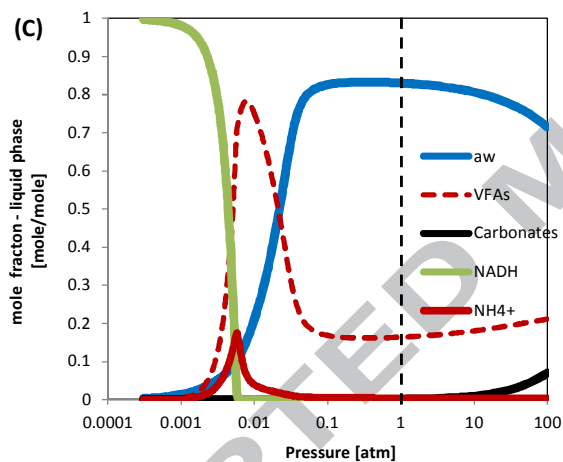
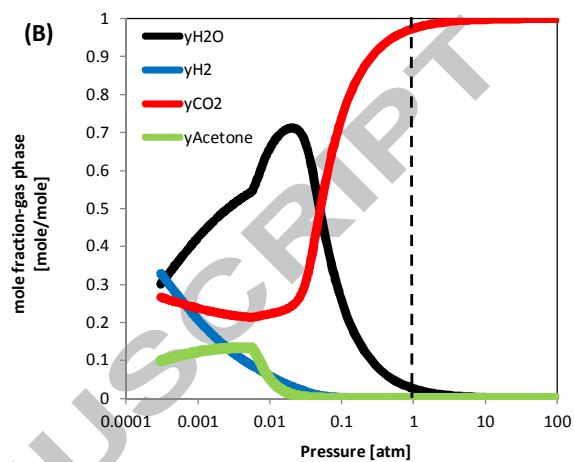
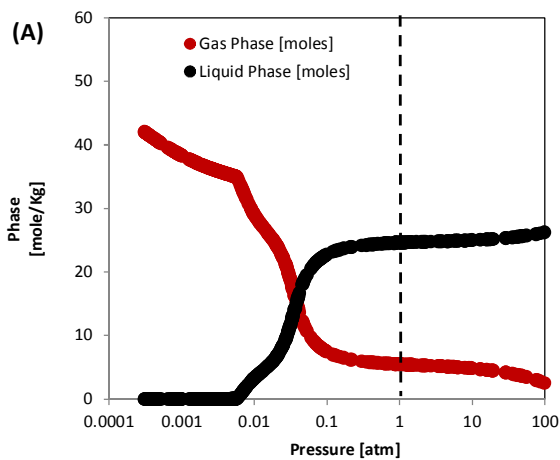


FIGURE 4. Pressure dependence in biotransformation of maltose with 2 mole kg^{-1} of maltose feedstock at 298.15 K, where a concentration dependence of maltose feedstock was studied at the dot line; (A) phase transition, (B) mole-fraction in the gas phase (C) mole-fraction in liquid phase, (D) individual mole-fractions of VFAs in the liquid phase, (E) pH value and NAD^+/NADH ratio and (F) enthalpy change and water production

ACCEPTED MANUSCRIPT

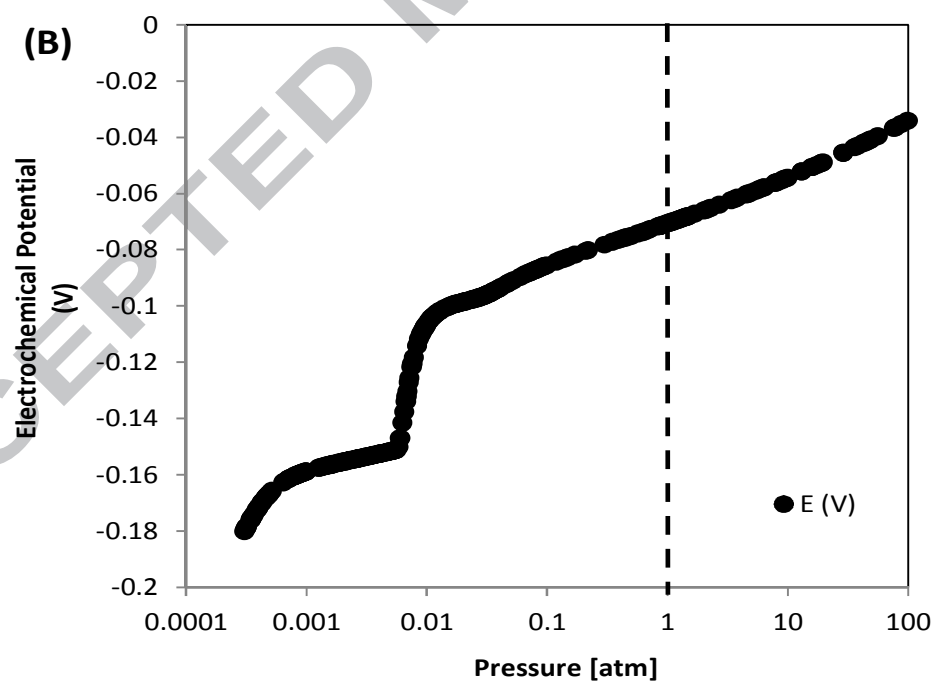
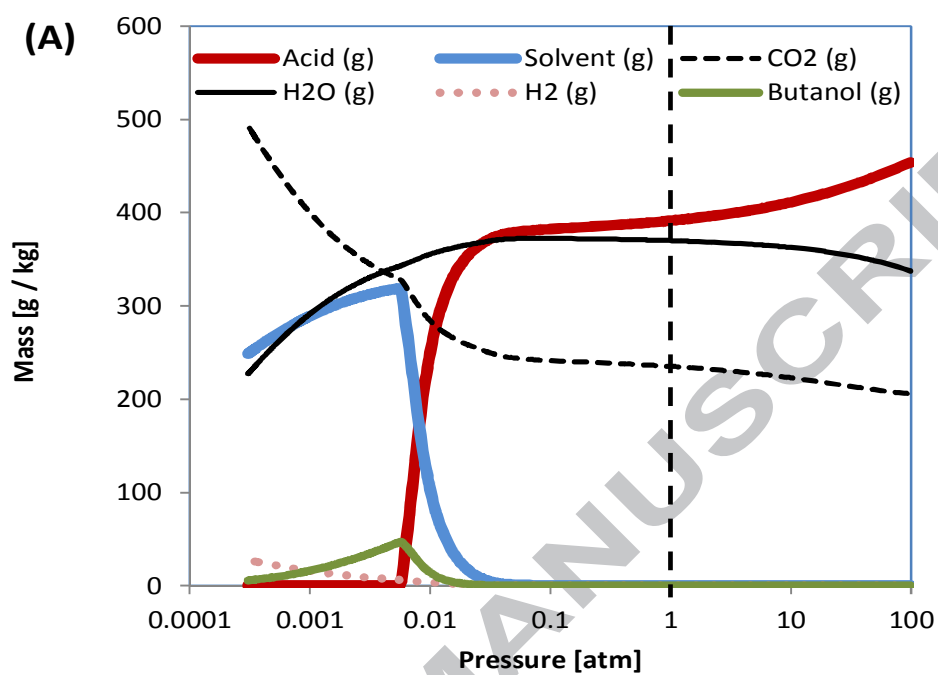


FIGURE 5. Pressure dependence in biotransformation of maltose with 2 mole kg⁻¹ of maltose feedstock at 298.15 K, where a concentration dependence of maltose feedstock was studied at the dot line; (A) mass balance and (B) electrochemical potential

ACCEPTED MANUSCRIPT

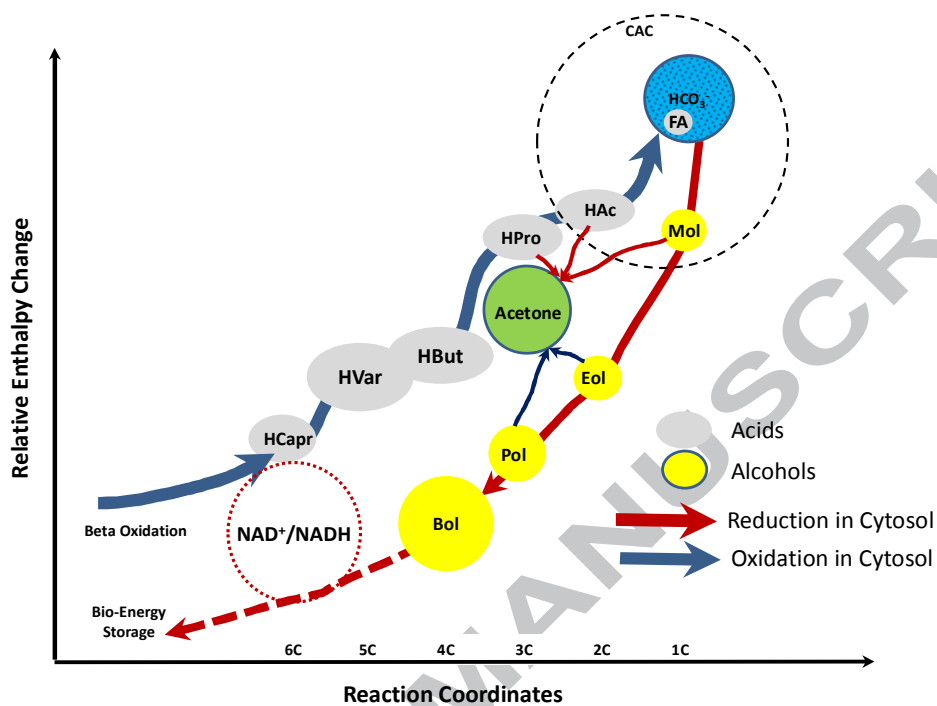


FIGURE 6. Reactions coordinate of beta-oxidation (catabolism) with energy storage (biosynthesis) at the starvation of carbohydrates

TABLE CAPTIONS

TABLE 1. Stoichiometric model of biotransformation of maltose

TABLE 2. Phase equilibria of biotransformation of maltose

TABLE 3. Dissociation equilibria of biotransformation of maltose

TABLE 4. Electrochemical equilibria of biotransformation of maltose

ACCEPTED MANUSCRIPT

TABLE 1. Stoichiometric model of biotransformation of maltose

Phase transitions (gas aq)	Electrolyte relations	Electrochemical half reactions
$\text{H}_2\text{O}(\text{g}) \rightleftharpoons \text{H}_2\text{O}(\text{l})$ $\text{H}_2(\text{g}) \rightleftharpoons \text{H}_2(\text{aq})$	$\text{H}_2\text{O}(\text{l}) \rightleftharpoons \text{H}^+ + \text{OH}^-$	$\text{NADH} + \text{H}^+ \rightleftharpoons \text{NAD}^+ + 2\text{H}^+ + 2\text{e}^-$ $\text{H}_2(\text{g}) \rightleftharpoons 2\text{H}^+ + 2\text{e}^-$
$\text{NH}_3(\text{g}) \rightleftharpoons \text{NH}_3(\text{aq})$ $\text{N}_2(\text{g}) \rightleftharpoons \text{N}_2(\text{aq})$	$\text{NH}_3(\text{aq}) + \text{H}_2\text{O} \rightleftharpoons \text{NH}_4^+ + \text{OH}^-$ $\text{NH}_3(\text{aq}) + \text{H}_2\text{O} \rightleftharpoons \text{NH}_4\text{OH}$ $\text{HNO}_2 \rightleftharpoons \text{NO}_2^- + \text{H}^+$ $\text{HNO}_3 \rightleftharpoons \text{NO}_3^- + \text{H}^+$ $\text{NH}_4\text{NO}_3 \rightleftharpoons \text{NH}_4^+ + \text{NO}_3^-$	$2\text{NH}_3(\text{g}) \rightleftharpoons \text{N}_2(\text{g}) + 6\text{H}^+ + 6\text{e}^-$ $\text{NH}_3(\text{g}) + 2\text{H}_2\text{O} \rightleftharpoons \text{NO}_2^- + 7\text{H}^+ + 6\text{e}^-$ $\text{NO}_2^- + \text{H}_2\text{O} \rightleftharpoons \text{NO}_3^- + 2\text{H}^+ + 2\text{e}^-$
$\text{CO}_2(\text{g}) \rightleftharpoons \text{CO}_2(\text{aq})$	$\text{CO}_2(\text{aq}) + \text{H}_2\text{O} \rightleftharpoons \text{H}_2\text{CO}_3$ $\text{CO}_2(\text{aq}) + \text{H}_2\text{O} \rightleftharpoons \text{HCO}_3^- + \text{H}^+$ $\text{CO}_2(\text{aq}) + \text{H}_2\text{O} \rightleftharpoons \text{CO}_3^{2-} + 2\text{H}^+$ $(\text{NH}_4)\text{HCO}_3 \rightleftharpoons \text{NH}_3(\text{g}) + \text{CO}_2(\text{g}) + \text{H}_2\text{O}$ $(\text{NH}_4)_2\text{CO}_3 \rightleftharpoons 2\text{NH}_3(\text{g}) + \text{CO}_2(\text{g}) + \text{H}_2\text{O}$ $\text{NH}_3(\text{aq}) + \text{HCO}_3^- \rightleftharpoons \text{NH}_2\text{CO}_2^- + \text{H}_2\text{O}$	
	$\text{CH}_2\text{O}_2(\text{aq}) \rightleftharpoons \text{CHO}_2^- + \text{H}^+$ $\text{C}_2\text{H}_4\text{O}_2(\text{aq}) \rightleftharpoons \text{C}_2\text{H}_3\text{O}_2^- + \text{H}^+$ $\text{C}_3\text{H}_6\text{O}_2(\text{aq}) \rightleftharpoons \text{C}_3\text{H}_5\text{O}_2^- + \text{H}^+$ $\text{C}_4\text{H}_8\text{O}_2(\text{aq}) \rightleftharpoons \text{C}_4\text{H}_7\text{O}_2^- + \text{H}^+$ $\text{C}_5\text{H}_{10}\text{O}_2(\text{aq}) \rightleftharpoons \text{C}_5\text{H}_9\text{O}_2^- + \text{H}^+$ $\text{C}_6\text{H}_{12}\text{O}_2(\text{aq}) \rightleftharpoons \text{C}_6\text{H}_{11}\text{O}_2^- + \text{H}^+$ $\text{C}_3\text{H}_4\text{O}_3(\text{aq}) \rightleftharpoons \text{C}_3\text{H}_3\text{O}_3^- + \text{H}^+$ $\text{C}_3\text{H}_6\text{O}_3(\text{aq}) \rightleftharpoons \text{C}_3\text{H}_5\text{O}_3^- + \text{H}^+$ $\text{C}_4\text{H}_6\text{O}_4(\text{aq}) \rightleftharpoons \text{C}_4\text{H}_5\text{O}_4^- + \text{H}^+$ $\text{C}_4\text{H}_6\text{O}_4(\text{aq}) \rightleftharpoons \text{C}_4\text{H}_4\text{O}_4^- + 2\text{H}^+$	$\text{CH}_2\text{O}_2(\text{aq}) \rightleftharpoons \text{CO}_2(\text{g}) + 2\text{H}^+ + 2\text{e}^-$ $\text{C}_2\text{H}_4\text{O}_2(\text{aq}) + 2\text{H}_2\text{O} \rightleftharpoons 2\text{CO}_2(\text{g}) + 8\text{H}^+ + 8\text{e}^-$ $\text{C}_3\text{H}_6\text{O}_2(\text{aq}) + 2\text{H}_2\text{O} \rightleftharpoons \text{C}_2\text{H}_4\text{O}_2(\text{aq}) + \text{CO}_2(\text{g}) + 6\text{H}^+ + 6\text{e}^-$ $\text{C}_4\text{H}_8\text{O}_2(\text{aq}) + 2\text{H}_2\text{O} \rightleftharpoons 2\text{C}_2\text{H}_4\text{O}_2(\text{aq}) + 4\text{H}^+ + 4\text{e}^-$ $\text{C}_5\text{H}_{10}\text{O}_2(\text{aq}) + 2\text{H}_2\text{O} \rightleftharpoons \text{C}_2\text{H}_4\text{O}_2(\text{aq}) + \text{C}_3\text{H}_6\text{O}_2(\text{aq}) + 4\text{H}^+ + 4\text{e}^-$ $\text{C}_6\text{H}_{12}\text{O}_2(\text{aq}) + 2\text{H}_2\text{O} \rightleftharpoons \text{C}_2\text{H}_4\text{O}_2(\text{aq}) + \text{C}_4\text{H}_8\text{O}_2(\text{aq}) + 4\text{H}^+ + 4\text{e}^-$ $\text{C}_3\text{H}_6\text{O}_2(\text{aq}) + \text{H}_2\text{O} \rightleftharpoons \text{C}_3\text{H}_4\text{O}_3(\text{aq}) + 4\text{H}^+ + 4\text{e}^-$ $\text{C}_3\text{H}_6\text{O}_2(\text{aq}) + \text{H}_2\text{O} \rightleftharpoons \text{C}_3\text{H}_6\text{O}_3(\text{aq}) + 2\text{H}^+ + 2\text{e}^-$ $\text{C}_4\text{H}_8\text{O}_2(\text{aq}) + 2\text{H}_2\text{O} \rightleftharpoons \text{C}_4\text{H}_6\text{O}_4(\text{aq}) + 6\text{H}^+ + 6\text{e}^-$

Continuing Table 1

Phase transitions (gas aq)	Electrolyte relations	Electrochemical half reactions
	$C_3H_8O_3 (aq) \rightleftharpoons C_3H_6O_2 (aq) + H_2O$ $C_4H_6O_5 (aq) \rightleftharpoons C_4H_5O_5^- + H^+$ $C_4H_6O_5 (aq) \rightleftharpoons C_4H_4O_5^- + 2H^+$ $C_6H_8O_7 (aq) \rightleftharpoons C_6H_7O_7^- + H^+$ $C_6H_8O_7 (aq) \rightleftharpoons C_6H_6O_7^- + 2H^+$ $C_6H_8O_7 (aq) \rightleftharpoons C_6H_5O_7^- + 3H^+$ $CH_2O_2(NH_4) \rightleftharpoons NH_3(g) + CH_2O_2 (aq)$ $C_2H_3O_2(NH_4) \rightleftharpoons NH_3(g) + C_2H_4O_2 (aq)$	$C_4H_6O_4 (aq) + H_2O \rightleftharpoons C_4H_6O_5 (aq) + 2H^+ + 2e^-$ $C_6H_8O_7 (aq) + H_2O \rightleftharpoons C_4H_6O_4 (aq) + 2CO_2(g) + 4H^+ + 4e^-$
$CH_4O (g) \rightleftharpoons CH_4O (aq)$ $C_2H_4O (g) \rightleftharpoons C_2H_4O (aq)$ $C_2H_6O (g) \rightleftharpoons C_2H_6O (aq)$ $C_3H_6O (g) \rightleftharpoons C_3H_6O (aq)$ $n-C_3H_8O (g) \rightleftharpoons n-C_3H_8O (aq)$ $iso-C_3H_8O (g) \rightleftharpoons iso-C_3H_8O (aq)$ $n-C_4H_{10}O (g) \rightleftharpoons n-C_4H_{10}O (aq)$ $iso-C_4H_{10}O (g) \rightleftharpoons iso-C_4H_{10}O (aq)$ $sec-C_4H_{10}O (g) \rightleftharpoons sec-C_4H_{10}O (aq)$ $Tert-C_4H_{10}O (g) \rightleftharpoons Tert-C_4H_{10}O (aq)$		$CH_4O (aq) + H_2O \rightleftharpoons CO_2 (g) + 6H^+ + 6e^-$ $C_2H_6O (aq) \rightleftharpoons C_2H_4O (aq) + 2H^+ + 2e^-$ $C_2H_6O (aq) + H_2O \rightleftharpoons C_2H_4O_2 (aq) + 4H^+ + 4e^-$ $C_3H_6O (aq) + H_2O \rightleftharpoons C_3H_6O_2 (aq) + 2H^+ + 2e^-$ $n-C_3H_8O (aq) + H_2O \rightleftharpoons C_3H_6O_2 (aq) + 4H^+ + 4e^-$ $iso-C_3H_8O (aq) + H_2O \rightleftharpoons C_3H_6O_2 (aq) + 4H^+ + 4e^-$ $n-C_4H_{10}O (aq) + H_2O \rightleftharpoons C_4H_8O_2 (aq) + 4H^+ + 4e^-$ $iso-C_4H_{10}O (aq) + H_2O \rightleftharpoons C_4H_8O_2 (aq) + 4H^+ + 4e^-$ $sec-C_4H_{10}O (aq) + H_2O \rightleftharpoons C_4H_8O_2 (aq) + 4H^+ + 4e^-$ $tetra-C_4H_{10}O (aq) + H_2O \rightleftharpoons C_4H_8O_2 (aq) + 4H^+ + 4e^-$ $C_4H_8O_2 (aq) + C_2H_4O_2 (aq) + 2H_2O \rightleftharpoons C_6H_{12}O_6 (aq) + 4H^+ + 4e^-$
	$C_{12}H_{22}O_{11} (maltose) + H_2O \rightleftharpoons 2 C_6H_{12}O_6 (aq)$	

TABLE 2. Phasic equilibria of biotransformation of maltose

Vapour-liquid (Water) Equilibria		Equilibrium Reaction	Equation	Common Name	Equilibrium Constants $\log(K_{i-W}^H)$
		$H_2O(g) = H_2O(l)$	$y_W \Phi_W P = \Phi_W^{sat} P_W^{sat} \exp \left[\int_{P_W^{sat}}^P \frac{\bar{v}_{H_2O}^{Liquid}}{RT} dp \right]$	Water	1.5
		$H_2(g) = H_2(aq)$	$y_{H_2} \Phi_{H_2} P = m_{H_2} K_{H_2-W}^H \exp \left[\int_{P_{H_2}^{sat}}^P \frac{\bar{v}_{H_2-W}}{RT} dp \right]$	Hydrogen	-3.07
		$CO_2(g) = CO_2(aq)$	$y_{CO_2} \Phi_{CO_2} P = m_{CO_2} K_{CO_2-W}^H \exp \left[\int_{P_{CO_2}^{sat}}^P \frac{\bar{v}_{CO_2-W}}{RT} dp \right]$	Carbon dioxide	-1.34
		$NH_3(g) = NH_3(aq)$	$y_{NH_3} \Phi_{NH_3} P = m_{NH_3} K_{NH_3-W}^H \exp \left[\int_{P_{NH_3}^{sat}}^P \frac{\bar{v}_{NH_3-W}}{RT} dp \right]$	Ammonia	1.74
		$N_2(g) = N_2(aq)$	$y_{N_2} \Phi_{N_2} P = m_{N_2} K_{N_2-W}^H \exp \left[\int_{P_{N_2}^{sat}}^P \frac{\bar{v}_{N_2-W}}{RT} dp \right]$	Nitrogen	-3.17
		$CH_4O(g) = CH_4O(aq)$	$y_{CH_4O} \Phi_{CH_4O} P = m_{CH_4O} K_{CH_4O-W}^H \exp \left[\int_{P_{CH_4O}^{sat}}^P \frac{\bar{v}_{CH_4O-W}}{RT} dp \right]$	Methanol	2.22
		$C_2H_4O(g) = C_2H_4O(aq)$	$y_{C_2H_4O} \Phi_{C_2H_4O} P = m_{C_2H_4O} K_{C_2H_4O-W}^H \exp \left[\int_{P_{C_2H_4O}^{sat}}^P \frac{\bar{v}_{C_2H_4O-W}}{RT} dp \right]$	Acetaldehyde	1.14
		$C_2H_6O(g) = C_2H_6O(aq)$	$y_{Ethanol} \Phi_{Ethanol} P = m_{Ethanol} K_{Ethanol-W}^H \exp \left[\int_{P_{Ethanol}^{sat}}^P \frac{\bar{v}_{Ethanol-W}}{RT} dp \right]$	Ethanol	2.22
		$C_3H_6O(g) = C_3H_6O(aq)$	$y_{Acetone} \Phi_{Acetone} P = m_{Acetone} K_{Acetone-W}^H \exp \left[\int_{P_{Acetone}^{sat}}^P \frac{\bar{v}_{Acetone-W}}{RT} dp \right]$	Acetone	1.42
		$n-C_3H_8O(g) = n-C_3H_8O(aq)$	$y_{n-Pro} \Phi_{n-Pro} P = m_{n-Pro} K_{n-Pro-W}^H \exp \left[\int_{P_{n-Pro}^{sat}}^P \frac{\bar{v}_{n-Pro-W}}{RT} dp \right]$	n-Propanol	2.18
		$iso-C_3H_8O(g) = iso-C_3H_8O(aq)$	$y_{Iso-Pro} \Phi_{Iso-Pro} P = m_{Iso-Pro} K_{Iso-Pro-W}^H \exp \left[\int_{P_{Iso-Pro}^{sat}}^P \frac{\bar{v}_{Iso-Pro-W}}{RT} dp \right]$	iso-Propanol	2.05
		$n-C_4H_{10}O(g) = n-C_4H_{10}O(aq)$	$y_{n-But} \Phi_{n-But} P = m_{n-But} K_{n-But-W}^H \exp \left[\int_{P_{n-But}^{sat}}^P \frac{\bar{v}_{n-But-W}}{RT} dp \right]$	n-Butanol	2.16
		$iso-C_4H_{10}O(g) = iso-C_4H_{10}O(aq)$	$y_{iso-But} \Phi_{iso-But} P = m_{iso-But} K_{iso-But-W}^H \exp \left[\int_{P_{iso-But}^{sat}}^P \frac{\bar{v}_{iso-But-W}}{RT} dp \right]$	iso-Butanol	1.96
		$sec-C_4H_{10}O(g) = sec-C_4H_{10}O(aq)$	$y_{sec-But} \Phi_{sec-But} P = m_{sec-But} K_{sec-But-W}^H \exp \left[\int_{P_{sec-But}^{sat}}^P \frac{\bar{v}_{sec-But-W}}{RT} dp \right]$	sec-Butanol	1.99
		$Tert-C_4H_{10}O(g) = Tert-C_4H_{10}O(aq)$	$y_{Tert-But} \Phi_{Tert-But} P = m_{Tert-But} K_{Tert-But-W}^H \exp \left[\int_{P_{Tert-But}^{sat}}^P \frac{\bar{v}_{Tert-But-W}}{RT} dp \right]$	Tert-Butanol	1.87

Note: m is molarity in liquid phase, $\log(K_{i-W}^H)$ at 298.15K is calculated by Pourbaix's method [1] and evaluated by chemical properties handbook [2]. \bar{v}_{i-W}^{∞} is calculated by Nakamura's method [3], y and Φ_i are mole fraction and fugacity activity in gas phase.

TABLE 3. Dissociation equilibria of biotransformation of maltose

Equilibrium Reaction	Equation	equilibrium constants log(K _a)
$H_2O = H^+ + OH^-$	$K_w = m_{H^+} m_{OH^-} / a_{H_2O}$	-14.00
$CO_2(aq) + H_2O = H_2CO_3$	$K_{CO_2} = m_{H_2CO_3} / m_{CO_2} a_{H_2O}$	-4.38x10 ⁻²
$CO_2(aq) + H_2O = HCO_3^- + H^+$	$K_{H_2CO_3} = m_{HCO_3^-} m_{H^+} / m_{CO_2} a_{H_2O}$	-6.37
$CO_2(aq) + H_2O = CO_3^{2-} + 2H^+$	$K_{HCO_3^-} = m_{CO_3^{2-}} m_{H^+}^2 / m_{CO_2} a_{H_2O}$	-16.70
$CH_2O_2(aq) = CHO_2^- + H^+$	$K_{HC1} = m_{HC1^-} m_{H^+} / m_{HC1}$	-3.74
$C_2H_4O_2(aq) = C_2H_3O_2^- + H^+$	$K_{HC2} = m_{HC2^-} m_{H^+} / m_{HC2}$	-4.76
$C_3H_6O_2(aq) = C_3H_5O_2^- + H^+$	$K_{HC3} = m_{HC3^-} m_{H^+} / m_{HC3}$	-4.87
$C_4H_8O_2(aq) = C_4H_7O_2^- + H^+$	$K_{HC4} = m_{HC4^-} m_{H^+} / m_{HC4}$	-4.82
$C_5H_{10}O_2(aq) = C_5H_9O_2^- + H^+$	$K_{HC5} = m_{HC5^-} m_{H^+} / m_{HC5}$	-4.67
$C_6H_{12}O_2(aq) = C_6H_{11}O_2^- + H^+$	$K_{HC6} = m_{HC6^-} m_{H^+} / m_{HC6}$	-4.85
$C_3H_4O_3(aq) = C_3H_3O_3^- + H^+$	$K_{C_3H_4O_3} = m_{C_3H_3O_3^-} m_{H^+} / m_{C_3H_4O_3}$	-2.49
$C_3H_6O_3(aq) = C_3H_5O_3^- + H^+$	$K_{C_3H_6O_3} = m_{C_3H_5O_3^-} m_{H^+} / m_{C_3H_6O_3}$	-3.86
$C_4H_6O_4(aq) = C_4H_5O_4^- + H^+$	$K_{C_4H_6O_4} = m_{C_4H_5O_4^-} m_{H^+} / m_{C_4H_6O_4}$	-4.20
$C_4H_6O_4(aq) = C_4H_4O_4^{2-} + 2H^+$	$K_{C_4H_6O_4} = m_{C_4H_4O_4^{2-}} m_{H^+}^2 / m_{C_4H_6O_4}$	-9.85
$C_4H_6O_5(aq) = C_4H_5O_5^- + H^+$	$K_{C_4H_6O_5} = m_{C_4H_5O_5^-} m_{H^+} / m_{C_4H_6O_5}$	-3.44
$C_4H_6O_5(aq) = C_4H_4O_5^{2-} + 2H^+$	$K_{C_4H_6O_5} = m_{C_4H_4O_5^{2-}} m_{H^+}^2 / m_{C_4H_6O_5}$	-7.97
$C_6H_8O_7(aq) = C_6H_7O_7^- + H^+$	$K_{C_6H_8O_7} = m_{C_6H_7O_7^-} m_{H^+} / m_{C_6H_8O_7}$	-3.07
$C_6H_8O_7(aq) = C_6H_6O_7^{2-} + 2H^+$	$K_{C_6H_8O_7} = m_{C_6H_6O_7^{2-}} m_{H^+}^2 / m_{C_6H_8O_7}$	-7.88
$C_6H_8O_7(aq) = C_6H_5O_7^{3-} + 3H^+$	$K_{C_6H_8O_7} = m_{C_6H_5O_7^{3-}} m_{H^+}^3 / m_{C_6H_8O_7}$	-14.28
$NH_3(aq) + H_2O = NH_4^+ + OH^-$	$K_{NH_3} = m_{NH_4^+} m_{OH^-} / m_{NH_3} a_{H_2O}$	-2.98
$NH_3(aq) + H_2O = NH_4OH$	$K_{NH_4OH} = m_{NH_4OH} / m_{NH_3} a_{H_2O}$	1.74
$NH_3(g) + CO_2(g) = (NH_2)CO_2^- + H^+$	$K_{(NH_2)CO_2} = m_{(NH_2)CO_2^-} m_{H^+} / y_{NH_3} y_{CO_2} \Phi_{NH_3} \Phi_{CO_2} P^2$	-19.94
$HNO_2(aq) = NO_2^- + H^+$	$K_{HNO_2} = m_{NO_2^-} m_{H^+} / m_{HNO_2}$	-3.35
$HNO_3(aq) = NO_3^- + H^+$	$K_{HNO_3} = m_{NO_3^-} m_{H^+} / m_{HNO_3}$	0
$NH_4NO_3(s) = NH_4^+ + NO_3^-$	$K_{NH_4NO_3} = m_{NH_4^+} m_{NO_3^-} / m_{NH_4NO_3}$	1.21
$(NH_4)HCO_3 = NH_3(g) + CO_2(g) + H_2O$	$K_{(NH_4)HCO_3} = y_{NH_3} y_{CO_2} \Phi_{NH_3} \Phi_{CO_2} P^2 \cdot a_{H_2O} / m_{(NH_4)HCO_3}$	-3.13
$(NH_4)_2CO_3 = 2NH_3(g) + CO_2(g) + H_2O$	$K_{(NH_4)_2CO_3} = y_{NH_3}^2 y_{CO_2} \Phi_{NH_3}^2 \Phi_{CO_2} P^3 \cdot a_{H_2O} / m_{(NH_4)_2CO_3}$	-3.78
$CHO_2(NH_4) = NH_3(g) + CH_2O_2(aq)$	$K_{(NH_4)HC1} = y_{NH_3} \Phi_{NH_3} P \cdot m_{HC1} / m_{(NH_4)HC1}$	-10.11
$C_2H_3O_2(NH_4) = NH_3(g) + C_2H_4O_2(aq)$	$K_{(NH_4)HC2} = y_{NH_3} \Phi_{NH_3} P \cdot m_{HC2} / m_{(NH_4)HC2}$	-4.88
$C_3H_8O_3(aq) = C_3H_6O_2(aq) + H_2O$	$K_{C_3H_8O_3} = m_{C_3H_6O_2} a_{H_2O} / m_{C_3H_8O_3}$	21.59
$C_{12}H_{22}O_{11}(\text{maltose}) + H_2O = 2 C_6H_{12}O_6(aq)$	$K_{Maltose} = m_{Glucose}^2 / m_{Maltose} a_{H_2O}$	3.86

Note: log(K_a) at 298.15K is calculated by Pourbaix's method [1] and evaluated by chemical properties handbook [2, 4]. Subscript HC1, HC2, HC3, HC4, HC5 and HC6 are represented as

metanoic, ethanoic, propanoic, butyric, pentanoic and hexanoic acids respectively. a_{H_2O} is the water activity.

ACCEPTED MANUSCRIPT

TABLE 4. Electrochemical equilibria of biotransformation of maltose

Microbial Reactions	Half reactions	Chemical Equilibrium constants log(K)	Electrochemical Potential (V)
<i>Biochemical Mediator</i>			
	$\text{NADH} + \text{H}^+ = \text{NAD}^+ + 2\text{H}^+ + 2\text{e}^-$	-3.12	0.0922
	$\text{H}_2 (\text{g}) = 2\text{H}^+ + 2\text{e}^-$	0	0
<i>Syntrophic Acetogenic and Acetoclastic Bacteria</i>			
	$\text{CH}_2\text{O}_2 (\text{aq}) = \text{CO}_2(\text{g}) + 2\text{H}^+ + 2\text{e}^-$	6.71	-0.1985
	$\text{C}_2\text{H}_4\text{O}_2(\text{aq}) + 2\text{H}_2\text{O} = 2\text{CO}_2(\text{g}) + 8\text{H}^+ + 8\text{e}^-$	-15.72	0.1162
	$\text{C}_3\text{H}_6\text{O}_2(\text{aq}) + 2\text{H}_2\text{O} = \text{C}_2\text{H}_4\text{O}_2 (\text{aq}) + \text{CO}_2 (\text{g}) + 6\text{H}^+ + 6\text{e}^-$	-10.41	0.1026
	$\text{C}_4\text{H}_8\text{O}_2(\text{aq}) + 2\text{H}_2\text{O} = 2\text{C}_2\text{H}_4\text{O}_2(\text{aq}) + 4\text{H}^+ + 4\text{e}^-$	-7.69	0.1137
	$\text{C}_5\text{H}_{10}\text{O}_2(\text{aq}) + 2\text{H}_2\text{O} = \text{C}_2\text{H}_4\text{O}_2(\text{aq}) + \text{C}_3\text{H}_6\text{O}_2(\text{aq}) + 4\text{H}^+ + 4\text{e}^-$	-10.13	0.1497
	$\text{C}_6\text{H}_{12}\text{O}_2(\text{aq}) + 2\text{H}_2\text{O} = \text{C}_2\text{H}_4\text{O}_2(\text{aq}) + \text{C}_4\text{H}_8\text{O}_2(\text{aq}) + 4\text{H}^+ + 4\text{e}^-$	-5.71	0.0844
<i>Acidogenic Bacteria</i>			
	$\text{CH}_4\text{O} (\text{aq}) + \text{H}_2\text{O} = \text{CO}_2 (\text{g}) + 6\text{H}^+ + 6\text{e}^-$	-3.16	0.0312
	$\text{C}_2\text{H}_6\text{O} (\text{aq}) + \text{H}_2\text{O} = \text{C}_2\text{H}_4\text{O}_2 (\text{aq}) + 4\text{H}^+ + 4\text{e}^-$	-2.46	0.0364
	$\text{n-C}_3\text{H}_8\text{O} (\text{aq}) + \text{H}_2\text{O} = \text{C}_3\text{H}_6\text{O}_2 (\text{aq}) + 4\text{H}^+ + 4\text{e}^-$	-2.82	0.0418
	$\text{iso-C}_3\text{H}_8\text{O} (\text{aq}) + \text{H}_2\text{O} = \text{C}_3\text{H}_6\text{O}_2 (\text{aq}) + 4\text{H}^+ + 4\text{e}^-$	-3.15	0.0466
	$\text{n-C}_4\text{H}_{10}\text{O} (\text{aq}) + \text{H}_2\text{O} = \text{C}_4\text{H}_8\text{O}_2 (\text{aq}) + 4\text{H}^+ + 4\text{e}^-$	-2.37	0.0350
	$\text{iso-C}_4\text{H}_{10}\text{O} (\text{aq}) + \text{H}_2\text{O} = \text{C}_4\text{H}_8\text{O}_2 (\text{aq}) + 4\text{H}^+ + 4\text{e}^-$	-2.79	0.0413
	$\text{sec-C}_4\text{H}_{10}\text{O} (\text{aq}) + \text{H}_2\text{O} = \text{C}_4\text{H}_8\text{O}_2 (\text{aq}) + 4\text{H}^+ + 4\text{e}^-$	-2.79	0.0413
	$\text{tetra-C}_4\text{H}_{10}\text{O} (\text{aq}) + \text{H}_2\text{O} = \text{C}_4\text{H}_8\text{O}_2 (\text{aq}) + 4\text{H}^+ + 4\text{e}^-$	-1.87	0.0276
	$\text{C}_2\text{H}_6\text{O} (\text{aq}) = \text{C}_2\text{H}_4\text{O} (\text{aq}) + 2\text{H}^+ + 2\text{e}^-$	-7.34	0.2170
	$\text{C}_3\text{H}_6\text{O} (\text{aq}) + \text{H}_2\text{O} = \text{C}_3\text{H}_6\text{O}_2 (\text{aq}) + 2\text{H}^+ + 2\text{e}^-$	-2.36	0.0693
	$\text{C}_4\text{H}_8\text{O}_2 (\text{aq}) + 2\text{H}_2\text{O} = \text{C}_4\text{H}_6\text{O}_4 (\text{aq}) + 6\text{H}^+ + 6\text{e}^-$	-18.48	0.1822
	$\text{C}_3\text{H}_6\text{O}_2 (\text{aq}) + \text{H}_2\text{O} = \text{C}_3\text{H}_6\text{O}_3 (\text{aq}) + 2\text{H}^+ + 2\text{e}^-$	-14.36	0.4245
	$\text{C}_3\text{H}_6\text{O}_2 (\text{aq}) + \text{H}_2\text{O} = \text{C}_3\text{H}_4\text{O}_3 (\text{aq}) + 4\text{H}^+ + 4\text{e}^-$	-23.50	0.3474
	$\text{C}_6\text{H}_8\text{O}_7 (\text{aq}) + \text{H}_2\text{O} = \text{C}_4\text{H}_6\text{O}_4 (\text{aq}) + 2\text{CO}_2 (\text{g}) + 4\text{H}^+ + 4\text{e}^-$	9.46	-0.1400
	$\text{C}_4\text{H}_6\text{O}_4 (\text{aq}) + \text{H}_2\text{O} = \text{C}_4\text{H}_6\text{O}_5 (\text{aq}) + 2\text{H}^+ + 2\text{e}^-$	-16.16	0.4778
<i>Fermentative Bacteria</i>			
	$\text{C}_4\text{H}_8\text{O}_2 (\text{aq}) + \text{C}_2\text{H}_4\text{O}_2 (\text{aq}) + 2\text{H}_2\text{O} = \text{C}_6\text{H}_{12}\text{O}_6 (\text{aq}) + 4\text{H}^+ + 4\text{e}^-$	-59.44	0.8789
<i>Overall ammonia oxidising Bacteria</i>			
	$2\text{NH}_3(\text{g}) = \text{N}_2(\text{g}) + 6\text{H}^+ + 6\text{e}^-$	-5.83	0.0575
<i>Ammonium oxidising bacteria (AOB)</i>			
	$\text{NH}_3(\text{g}) + 2\text{H}_2\text{O} = \text{NO}_2^- + 7\text{H}^+ + 6\text{e}^-$	-80.00	0.7886
<i>Nitrite-oxidising bacteria (NOB)</i>			
	$\text{NO}_2^- + \text{H}_2\text{O} = \text{NO}_3^- + 2\text{H}^+ + 2\text{e}^-$	-28.10	0.8312

Note: These constants were calculated by Pourbaix's method [1] at 298.15K.

ACCEPTED MANUSCRIPT

Reference

- [1] M. Pourbaix, Atlas of electrochemical equilibria in aqueous solutions, NACE Cebelcon., New York, 1974.
- [2] C.L. Yaws, Yaws' Handbook of Thermodynamic and Physical Properties of Chemical Compounds, Knovel2003.
- [3] Nakamura R, B. GJF, Prausnitz JM, Thermodynamic Properties of gas mixtures containing common polar and nonpolar components, Ind Eng, Chem Process Design Division 15 (1976) pp 557–564.
- [4] Carl. L. Yaws, Chemical Properties Handbook, 1 ed., McGraw Hill, New York, 1997.

ACCEPTED MANUSCRIPT

Highlights

- Microbial glycolysis does not occur together with CAC in batch digesters.
- Pressurised digester increased microbial CAC.
- Depressurised digester accumulated 'acetone' through 'butanol'

ACCEPTED MANUSCRIPT